Quantifying the influence of individual trees on slope stability at landscape scale

Raphael I. Spiekermann [a,b,*], Sam McColl [b], Ian Fuller [b], John Dymond [a], Lucy Burkitt [b], Hugh G. Smith [a]

[a] *Manaaki Whenua – Landcare Research, Palmerston North, New Zealand*
[b] *School of Agriculture and Environment, Massey University, Palmerston North, New Zealand*

ARTICLE INFO

ABSTRACT

Silvopastoralism in New Zealand's highly erodible hill country is an important form of erosion and sediment control. Yet, there has been little quantitative work to establish the effectiveness of space-planted trees in reducing shallow landslide erosion. We propose a method to provide high-resolution spatially explicit individual tree influence models at landscape scale for the dominant species in pastoral hill country. The combined hydrological and mechanical influence of trees on slopes is inferred through the spatial relationship between trees and landslide erosion. First, we delineate individual tree crowns and classify these into four dominant species classes found in New Zealand's pastoral hill country. This is the first species classification of individual trees at landscape scale in New Zealand using freely accessible data, achieving an overall accuracy of 92.6%. Second, we develop tree influence models for each species class by means of inductive inference. The inferred empirical tree influence models largely agree with the shape and distribution of existing physical root reinforcement models. Of exotic species that were planted for erosion and sediment control, poplars (*Populus* spp.) and willows (*Salix* spp.) make up 51% (109,000 trees) in pastoral hill country at a mean density of 3.2 trees/ha. In line with previous studies, poplars and willows have the greatest contribution to slope stability with an average maximum effective distance of 20 m. Yet, native kānuka (*Kunzea* spp.) is the most abundant woody vegetation species in pastoral hill country within the study area, with an average of 24.1 stems per ha (sph), providing an important soil conservation function. A large proportion (56% or 212.5 km^2) of pastoral hill-country in the study area remains untreated. The tree influence models presented in this study can be integrated into landslide susceptibility modelling in silvopastoral landscapes to both quantify the reduction in landslide susceptibility achieved and support targeted erosion and sediment mitigation plans.

1. Introduction

Woody vegetation significantly modifies hillslope hydrological and mechanical properties that control shallow landslide triggering processes and is an effective nature-based erosion mitigation instrument (Schmidt et al., 2001; Istanbulluoglu and Bras, 2005; Phillips and Marden, 2005; Schwarz et al., 2010a; Cohen and Schwarz, 2017; de Jesús Arce-Mojica et al., 2019). Several previous studies have aimed to quantify the influence of woody vegetation on slope stability, albeit mostly limited to protection forests (e.g. Phillips et al., 2011; Cislaghi et al., 2017). Irrespective of the type of woody vegetation, methods to quantify the effectiveness of biological landslide erosion control generally use i) empirical, ii) physical-, or iii) statistical-based approaches.

Quantitative empirical studies aim to measure the degree to which soil conservation treatment has reduced landslide erosion compared with untreated areas (Hawley and Dymond, 1988; Hicks, 1989a, b, 1992; Thompson and Luckman, 1993; Phillips et al., 2008; Douglas et al., 2009, 2013; McIvor et al., 2011, 2015). These studies show space-planted trees reduce landslide erosion by 70–95% within their assumed sphere of influence (e.g. a 10-m radius) compared with paired control sites.

Physical models of tree influence use quantitative measures for the mechanical and hydrological mechanisms of vegetation to estimate the increase in soil cohesion and slope stability achieved (e.g. Schmidt et al., 2001; Cohen et al., 2011; Schwarz et al., 2012; 2016; Moos et al., 2016; Gonzalez-Ollauri and Mickovski, 2017; Cislaghi et al., 2017). Physical

---

slope stability models that incorporate such measures of root reinforcement are sophisticated in replicating the processes governing slope stability, but their data requirements are significant, and extrapolation of measurements beyond individual sites is a challenge (Salvatici et al., 2018). Furthermore, root morphologies are modified by climatic and edaphic factors, which include physical soil conditions, resulting in highly variable root morphologies – even within a single species growing in different environments (Watson and O'Loughlin, 1990; Coppin and Richards, 1990; Stone and Kalisz, 1991; Phillips and Watson, 1994; Schmidt et al., 2001; Phillips and Marden, 2005). Therefore, physical slope stability models are generally used for landscapes with homogenous vegetation such as protection forests (e.g. Genet et al., 2010; Moos et al., 2016; Temgoua et al., 2016). The advantages of physical root distribution models, and their integration into slope stability models, was demonstrated by Schwarz et al. (2016), who determined optimal planting strategies using poplar trees for erosion control at hillslope scale for a New Zealand case study.

Statistical landslide susceptibility modelling is a common method used to disentangle the influence of a range of drivers that determine spatial variation in the probability of landsliding (Guzzetti et al., 2006; van Westen et al., 2008; Kanungo et al., 2009; Van Den Eeckhaut et al., 2009; Reichenbach et al., 2018; Knevels et al., 2020; Smith et al., 2021). In the absence of detailed vegetation classifications that would provide greater resolution in terms of the mechanical and hydrological mechanisms (e.g. root distribution models, canopy cover), land cover data are often used as surrogate datasets (Reichenbach et al., 2018). However, current land cover data are not at the resolution to account for the influence of space-planted trees in silvopastoral landscapes. Furthermore, simply representing individual trees as a point, mapping tree canopies, or using an arbitrary radius to define an area of influence of a tree, fails to acknowledge the spatial variation in the distribution and strength of roots in the soil as well as the influence on soil moisture.

In New Zealand, erosion processes are very active due to steep slopes, weak sedimentary rocks, high annual rainfall, and relatively frequent high magnitude rainfall events (Hicks et al., 2011; Basher, 2013). New Zealand's history of land management includes extensive deforestation for pastoral farming which has exacerbated erosion rates (Glade, 2003; Phillips et al., 2018). Given this setting, it is not surprising that most research on the impact of trees on landsliding in silvopastoral and agroforestry landscapes has been undertaken in New Zealand (England et al., 2020). Since the enactment of the Soil Conservation and Rivers Control Act 1941, which helped increase awareness for sustainable land management and soil conservation, spaced planting of trees has been an important erosion and sediment control measure (van Kraayenoord and Hathaway, 1986; Phillips et al., 2000, 2008; Basher et al., 2008, 2013), whereby poplars (*Populus* spp.) and willows (*Salix* spp.) are planted as young, unrooted stems (poles) at densities ranging from 20 to 200 trees ha^{-1} (Wilkinson, 1999; Benavides et al., 2009; Kemp et al., 2018). The objective of this form of silvopastoralism is generally to protect infrastructure and conserve soils to reduce sediment yields and improve freshwater health (Basher et al., 2020). Space-planted trees also offer shade, shelter, quality fodder (especially during drought periods), and carbon sequestration (McIvor et al., 2011). Dominati et al. (2014) quantified the long-term costs and benefits of space-planted trees in a pastoral farming context using an ecosystem services approach and found that despite the decrease in pastoral production below tree canopy, planting is economically beneficial in the long term due to the reduction in erosion risk and the increase in provision of ecosystem services including forage from trees, wood, provision of shade and shelter for animals, and net carbon accumulation in wood.

Despite the widespread use of space-planted trees in New Zealand's pastoral hill country, there has been relatively little experimental or quantitative work to establish their effectiveness in reducing erosion in relation to factors such as tree species, planting density, slope gradients, and there are no published studies on their measured effect on sediment yield (Douglas et al., 2009; Basher, 2013). Nor is there any information

on their effectiveness over a range of different storm magnitudes. This is largely due to the lack of spatially explicit data on individual trees and their influence on slope stability. Therefore, it is difficult to determine the extent to which erosion and sediment control measures have targeted slopes susceptible to landslide erosion and prioritized treatment of susceptible hillslopes.

Root data collection for multiple species and age classes is time-consuming and costly, partly explaining the paucity of quantitative data on the effectiveness of space-planted trees on slope stability in silvopastoral landscapes (Hairiah et al., 2020). This study introduces an empirical method to fill the gap in scale between i) physical, process-based models that quantify root reinforcement for individual trees and slope stability at hillslope scale, and ii) landslide susceptibility modelling at regional scale using land cover data. The objectives are: 1) to delineate individual tree crowns (ITCs) at landscape scale and classify into dominant species classes found in New Zealand's pastoral hill country; and 2) develop a spatially explicit tree influence model for each species class by means of inductive inference. The tree influence models represent the combined hydrological and mechanical influence of trees on slopes, which is inferred through the spatial relationship between individual trees and landslide erosion.

2. Methods

2.1. Study area

The study area was chosen based on five criteria: i) availability of airborne LiDAR (Light Detection and Ranging); ii) recent occurrence of storm events that resulted in a high density of shallow landslides; iii) pastoral farming as the dominant land use; iv) spanning a range of rock types; and v) a significant history of soil conservation practices that has resulted in a silvopastoral landscape. Following an inspection of historic Google Earth imagery to examine evidence of widespread landsliding, an 843 km^2 area was selected in the Wairarapa, located in the south-east of the North Island of New Zealand (Fig. 1). Approximately 92% of this area, or 776 km^2, is used for pastoral farming.

The study area is primarily underlain by unconsolidated, tectonically deformed Pliocene-age mudstone and fine siltstone (Fig. 1). Much of the area is covered in a mantle of loess. These soils have a dense subsoil zone of low permeability that is the failure plane for many landslides (De Rose, 2012). A band of limestone forms the central and south-western part of the study area. The terrain has low to moderate relief (<150 m) that is intensely dissected, with narrow ridge and spur crests, hillslopes mostly between 15° and 35°, and narrow valley floors. Significant areas of colluvium (landslide debris) have accumulated along the base of many hillslopes, and in mid- and upper-slope hollows. Mean annual rainfall is 1100 mm, characterised by winter maxima and summer droughts. Long duration, low intensity rainfall is typical with low daily rainfall totals. However, landslide-generating storms have occurred frequently since climatic records began in the 1880s. Most of these storms do not have particularly high storm or daily rainfall totals (100–200 mm) but often occur when antecedent moisture conditions are high (De Rose, 2012; Basher et al., 2018).

The study area was affected by two storm events in March 2005 and July 2006, with a median recorded rainfall of 175 mm and 204 mm over 48 and 72 h, respectively. These events triggered thousands of landslides across the entire study area. Three further storms, in late July 2006, October 2006, and June 2009, were more localised events recorded at Hikawera station in the south of the study area – the highest magnitude in 2009 with 197 mm in 24 h, with a resulting landslide distribution that was also localised to just part of the study area (Fig. 7). Shallow, rapid slides and flows involving soil and regolith are the most common types of landslides in New Zealand and consist of small scars (50–100 m^2) and long narrow debris tails (Glade, 1998; Crozier, 2005; Basher, 2013). Such landslides are generally triggered either by single, high-intensity and -magnitude rainfall events or by low-magnitude rainfall events
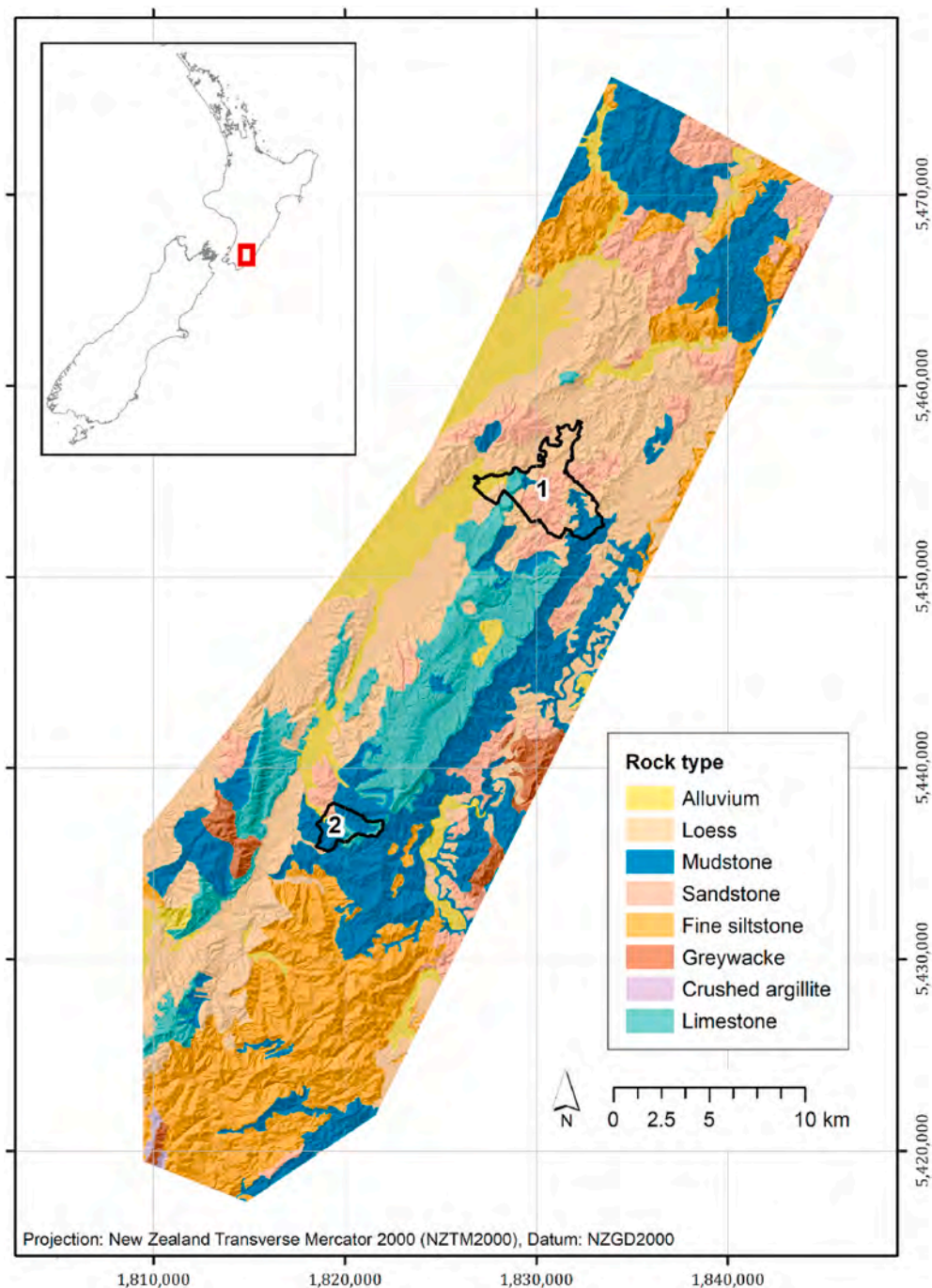
Fig. 1. Location of study area in Wairarapa, New Zealand, showing a range of rock types (New Zealand Land Resource Inventory) and location of study sites 1 and 2. Map projection is New Zealand Transverse Mercator (NZTM).

following prolonged wet periods that led to high antecedent soil moisture conditions (Basher, 2013).

2.2. Landslide mapping

To evaluate the influence of trees on slope stability at the study site, rainfall-triggered landslide scars were mapped. To do this for the storm events captured in this study, a semi-automated mapping procedure, using an object-based image analysis (OBIA) method was applied to identify and classify landslide scar features assumed to have been triggered in the 2005 and later storm events in the study area (Fig. 2). The OBIA method combines image processing and GIS functions to delineate and classify homogenous objects (Blaschke, 2010; Blaschke et al., 2014).

The primary advantage of this approach over manual delineation of scars is that it enables rapid mapping using a set of defined rules that ensures consistency across complete study areas. We used Trimble's eCognition software and employed a knowledge-based ruleset (Hölbling et al., 2016; Smith et al., 2021) (Fig. 2).

Landslide scars were classified in the 2010 imagery provided by Greater Wellington Regional Council, which is 3-band (RGB) optical imagery at 0.4 m ground space distance (GSD). Following a comparison with QuickBird II imagery from 30/01/2008, it was evident that the landslide scars triggered by the 2005 and 2006 rainfall events had not revegetated and could successfully be classified in the 2010 imagery. This visual inspection is supported by data on pasture dry matter production on slip scars by Lambert et al. (1984) and Rosser and Ross,
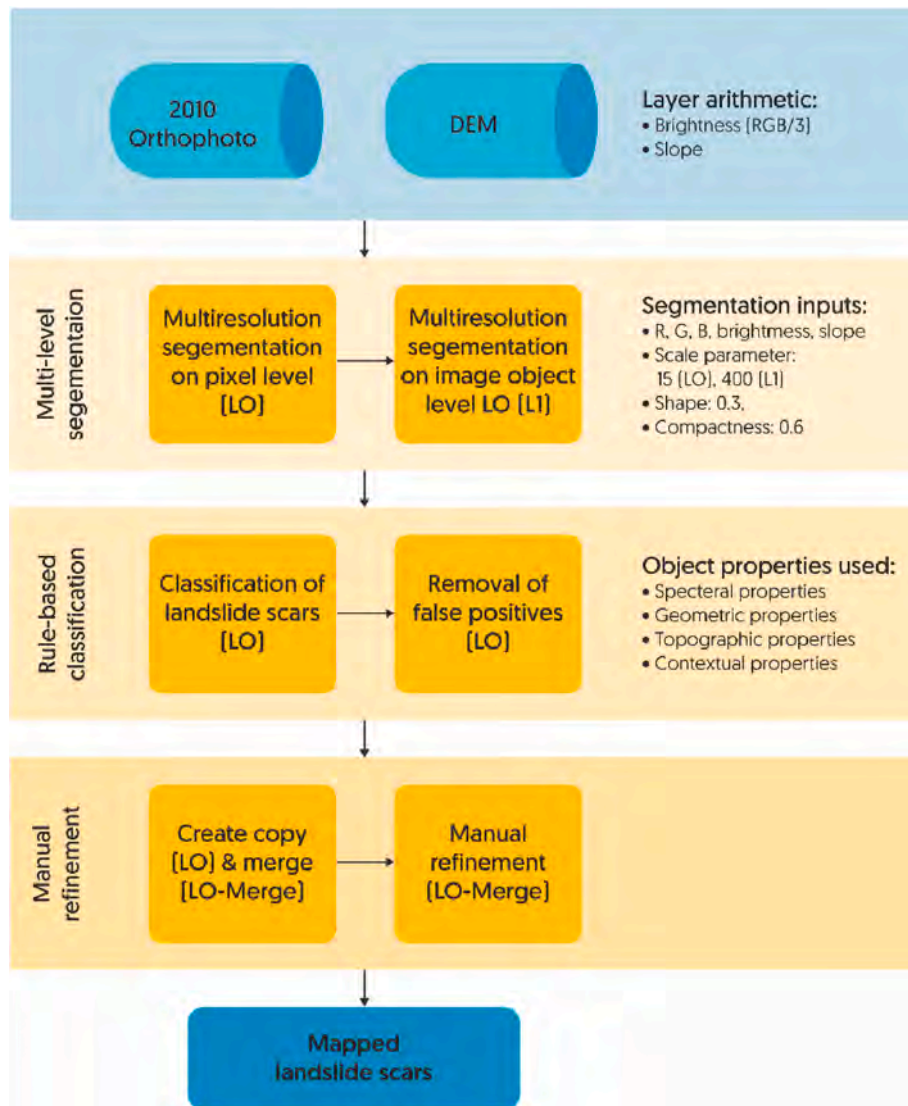
Fig. 2. Workflow for OBIA mapping of shallow landslide scars across study area.

(2011), who found pasture production at ~20% of the yields produced on uneroded ground, which was estimated to increase to ~30% after 5 years. There was a marked difference in the southern part of the study area, where scars triggered by the local event in 2009 were more clearly visible since revegetation of exposed regolith was not as advanced.

The 2010 RGB imagery was resampled to 1 m – the resolution of the LiDAR DEM. Image objects were created using the multiresolution segmentation algorithm based on spectral information of the imagery (i.e. identifying bright scars stripped of vegetation) and slope derived from the LiDAR DEM (i.e. to set topographic rules for realistic landslide geometries and slope locations). The landslide classification used two object levels in a multi-scaled segmentation approach, which organizes the objects into a hierarchy (Blaschke et al., 2014). The level 0 objects (L0) were created at the pixel level (1-m spatial resolution), whereby scale, shape and compactness parameters were optimized until image objects represented small landslide scars or components of larger landslides. The level 1 objects (L1) were generated through a second multi-resolution segmentation based on the L0 objects. This generally resulted in the delineation of individual paddocks/land parcels, which are related to the topology of the underlying L0 objects (Blaschke et al., 2014). The advantage of this approach is that the characterisation of low-level objects is enhanced through consideration of their local environmental setting (contextual properties). This was achieved by calculating the ratio and the mean difference in brightness between L0 and L1, which increases local contrast and removes significant errors (false positives/negatives) that occur when thresholds are set for complete study areas. Thus, for the classification of landslide scars at L0, scars were defined using i) mean brightness >140, ii) a ratio to L1 mean brightness >1, and iii) mean slope >20°. An automated procedure aimed at removing false positives by considering geometric (e.g. length, length/width ratio) and topographic (e.g. standard deviation of slope, elevation range) properties of image objects as well as objects less than 20 square metres in size, since it was difficult to verify on-screen whether or not these small objects were landslide scars. Further object-based manual refinement of the classification was performed across the entire study area by selecting and removing falsely classified objects. The age of most of the landslide scars (4–5 years since failure) meant there was less local contrast to surrounding non-landslide pixels than would otherwise be expected, and consequently, an unusually high number of false positives were classified as landslides. Most of the false positives were associated with bright objects such as farm tracks, areas of dry pasture, or exposed stream beds. 27 objects identified as landslide scars with areas >1500 m^2 were removed, as these were mostly components of actively eroding gully systems. This resulted in a dataset of 43,069 landslide scars.

2.3. Rural tree species classification

Two farms were selected for mapping tree species to generate the ground data required for training the support vector machine (SVM) classifier (Fig. 1). Both farms have a history of landslide and soil erosion research activity (e.g. Lambert et al., 1984, 1993; De Rose, 2012; Douglas et al., 2013; Basher et al., 2018). Site 1 is a 1700-ha sheep and beef farm, located approximately 15 km east of Masterton, in a region of steep pastoral hill country underlain by erodible Tertiary siltstones, mudstones, as well as some limestone. Here, the original landcover was predominantly podocarp-hardwood native vegetation that was cleared between 1860 and 1890 (Lambert et al., 1984). Soil conservation works in the form of space-planted poplar, willow, and eucalyptus trees began in the late 1990s. While planting has been sustained since commencement, the density of trees on hillslopes differs across the farm and is less than Site 2 (Fig. 3).

Site 2 is a 462-ha block of a sheep and beef farm located at the upper catchment of the Waikoukou Stream, a tributary of the Wangaehu, and has been continuously active in soil and water conservation since 1956. The main objectives of these conservation works were to intensively plant slopes and gullies prone to severe erosion using poplars, willows, and protected seedlings, install regulating dams to restrict peak flows and sediment loads entering waterways, and establish conservation woodlots in areas of severe gully and earthflow erosion. The original land cover likely consisted of light bush, kānuka, and fern with heavier podocarp species in the wider valleys. Several bush remnants of kānuka remain distributed across the farm. Soils are silt loam derived from mudstone and are generally typical of the soils found in the wider study area.

Tree mapping was carried out in the field at Sites 1 and 2 following two primary objectives: 1) to identify tree species to be used as samples in the tree species classification, and 2) to count the number of stems in selected densely-planted stands across different species classes (Table 1). Trees were mapped on printed sheets of aerial photography (2013/14) at a scale of 1:2500. Site visits found four dominant classes of tree species in paddocks used for pasture: poplar (*Populus* spp.) and

Table 1
Tree samples (count, %) used for rural tree species classification.

	Eucalyptus	Kānuka	Poplar/willow	Conifer	Other	Total
Site 1	316	1387	2225	132	909	4969
Percentage of total	6%	28%	45%	3%	18%	100%
Site 2	632	1801	1598	1169	169	5369
Percentage of total	12%	34%	30%	22%	3%	100%
Total	948	3188	3823	1301	1078	10338
Percentage of total	9%	31%	37%	13%	10%	100%

Fig. 3. Space-planted trees (kānuka, poplars and willows on slopes, cabbage trees lower right) at Sites 1 (above) and 2 (below), showing a range of species: Pinus radiata, poplars/willows, kānuka, eucalyptus. Sustained efforts over prolonged periods have resulted in higher density of planting at Site 2.

willow (*Salix* spp.) varieties, eucalyptus (*Eucalyptus* spp., e.g. *Eucalyptus globulus*), kānuka (*Kunzea* spp.), and *Pinus radiata* (hereafter referred to as conifers) (Table 1). These species made up 90% of all species mapped at the two sites. These four classes therefore formed the basis of the rural tree species classification. Other less common species mapped include acacias, other coniferous species such as cedar, Douglas fir, and spruce, and species native to New Zealand such as tōtara, (*Podocarpus totara*) and cabbage trees (*Cordyline australis*). Kānuka are often found with other species such as mānuka. Due to their greater height (10–20 m), kānuka eventually forms the dominant canopy (Allen et al., 1992; Bergin et al., 1995; Smale et al., 1997; Mackay-Smith et al. (submitted), resulting in homogenous mature kānuka stands as observed at sites 1 and 2.

In 2013 and 2014, the Wellington Regional Council commissioned a LiDAR survey with a minimum point density of 1.3 pt/m², a mean of 5.8 pt/m², and a vertical accuracy of ±0.15 m over the Wellington region (812,000 ha). These high-frequency LiDAR pulses are reflected by tree canopies (first return) and other surfaces, including leaves, branches and ultimately the ground (generally the last return). The travel distance of the different returns is then calculated as a function of return time, which provides very accurate point measurements of elevation. These point clouds can be classified and interpolated to generate digital terrain models (DTM) and digital surface models (DSM). The difference between these elevation models is a canopy height model (CHM) (Lefsky et al., 1999). Since the advent of LiDAR point clouds and digital elevation models (DEMs), many algorithms have been developed for automated delineation of ITCs (e.g. Bunting and Lucas, 2006; Dalponte and Coomes, 2016; Zhen et al., 2016; Pirotti et al., 2017). Here, we used the pycrown algorithm developed by Zörner et al., (2018) to delineate ITCs in the study area using the LiDAR-derived DTM and CHM at 1 m GSD (Fig. 4). Pycrown first identifies local maxima in a circular moving window, which represent treetops in the CHM. These local maxima are used as the seeds from which ITCs are grown, whereby growth is restricted by four defined thresholds: i) a threshold below which a pixel cannot be a tree (*th_tree*); ii) a growing threshold to determine whether a pixel is added to the tree crown, which must be greater than the mean height of the current crown multiplied by this value (*th_seed*); iii) a second growing threshold, whereby a pixel is added to the crown if its height is greater than the current mean height of the region multiplied by this value (0–1) (*th_crown*); and iv) a maximum value of the crown diameter of a detected tree (*max_crown*). We used stem counts of different species from the field to optimize parameterization of pycrown for the trees in our study area. We refer to Zörner et al., (2018) for a more detailed explanation of parameterization.

The most important parameter of pycrown is the window size used for identifying treetops with local maxima, since it has significant implications on the number of seeds identified and, thus, crowns delineated. Besides *th_tree*, the remaining thresholds determine the final crown geometry. Experimentation with three window sizes (3, 4, 5) found that 5 m yielded optimal results for space-planted trees. Therefore, a radius of 5 m was chosen, as well as default thresholds for crown growth of 0.45 (*th_seed*) and 0.55 (*th_crown*). The radius *max_crown* was set to 8 m due to a slight spatial incongruence between the LiDAR dataset and the orthophotos, which is minimal at nadir and reaches a maximum offset with increasing off-nadir viewing angles. By limiting the crown radius, the calculation of crown statistics (brightness, NDVI) using the orthophotos (Fig. 4) is less likely to include adjacent pixels not associated with the crowns (e.g. pasture).

Through overlay of field-based species mapping with ITCs in a GIS environment, ITCs within Sites 1 and 2 were labelled according to the mapped species. Besides tree height and crown area derived from LiDAR data, zonal statistics on spectral data (mean, standard deviation of the mean (SD)) were calculated for each tree crown in the study area using freely available high resolution multi-spectral aerial photography from three surveys flown in 2010, 2013/14 and 2016/17 (Table 2) and used as predictors in the SVM model (Fig. 4). By including a multi-temporal
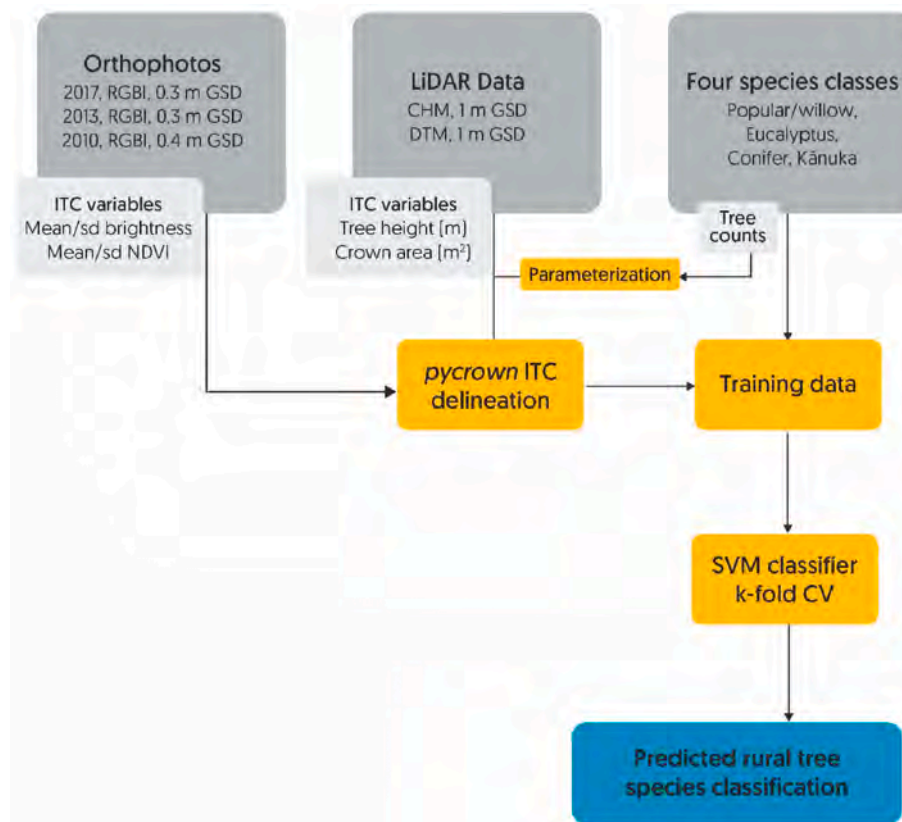

Fig. 4. Workflow and data inputs for rural tree species classification using an SVM model.

Table 2
Inputs derived from LiDAR data and optical imagery used in rural tree species classification.

Data	Model inputs	Variable abbreviation
Regional LiDAR 2013	1 Tree height (m)	TH
	2 Tree area (m^2)	Area
RGB 2010 imagery, 0.4 m GSD	3 Mean brightness	br_10_m
	4 Standard deviation brightness	br_10_sd
RGBI 2013/14 imagery, 0.3 m GSD	5 Mean brightness	br_13_m
	6 . Standard deviation brightness	br_13_sd
	7 Mean NDVI	ndvi_13_m
	8 Standard deviation NDVI	ndvi_13_sd
RGBI 2016/17 imagery, 0.3 m GSD	9 Mean brightness	br_17_m
	10 Standard deviation brightness	br_17_sd
	11 Mean NDVI	ndvi_17_m
	12 Standard deviation NDVI	ndvi_17_sd

dataset, seasonal variations in canopy characteristics improve the capability of the model to differentiate species. Furthermore, we hypothesised that including SDs as predictors would improve the model, since conifers and poplars/willows exhibit less spectral variance in the canopy than kānuka and eucalyptus. This compiled dataset was used as training and test data for an SVM model using the caret package (Kuhn, 2008) in R to develop a rural tree species classification of ITCs across the entire study area. SVM was originally developed as a binary classifier and later extended for multi-class classifications, and routinely outperforms more conventional approaches (Dalponte et al., 2012; Fassnacht et al. 2014, 2016; Dymond et al., 2019; Torabzadeh et al., 2019).

Using all 9260 tree crowns, we explored the best combinations of model inputs by performing 10-fold cross-validation, in which the data are randomly partitioned into ten equal sized subsamples and each subsample is used to test the remaining nine subsamples assigned to training. The 10-fold cross-validation was repeated 5 times with different random selections of subsamples to get an average overall classification accuracy, which we aim to maximise. For the identification of the best performing variables, parameters for cost penalty (=10) and σ (=0.05) were kept constant with a radial kernel function (RKF). Variable importance was evaluated using all training samples and receiver operating characteristic (ROC) curves and calculation of the area under curve (AUC). For multi-class outcomes, the problem is decomposed into all pair-wise problems and the AUC is calculated for each class pair. For a specific class, the maximum area under the curve across the relevant pair-wise AUCs is used as the variable importance measure. An AUC value of 0.5 corresponds to performance no better than a random guess, while an AUC of 1 would indicate perfect classification. Following variable selection, the final model tuned the hyperparameters of cost penalty and σ to achieve best performance, whereby a range of values for cost penalty (1:15) and σ (= 0.01,0.05,0.1) were tested. Model performance is characterised by overall accuracy (%) following 5 repeats of 10-fold cross-validation, and Cohen's Kappa, which accounts for expected accuracy resulting from uneven sample sizes across the classes (Cohen, 1960).

2.4. Empirical tree influence models on slope stability

The landslide database and tree classification were used in an empirical approach to quantify the influence of an individual tree on landslide activity. The method determines whether landslide scars occur preferentially close to or remote from trees. The overarching hypothesis is that by using spatial relationships and accounting for variability in the influencing factors, the influence of trees on landslide erosion may be inferred (Hawley and Dymond, 1988; Romeijn, 2009). Moreover, we assert that observations and patterns in the spatial distribution of tree

location and landslide erosion allow the physical properties of trees that govern slope stability to be inferred. This supposition may be verified through existing knowledge of physical properties of trees and root systems and the mechanisms by which trees increase slope stability (see section 4.2). The method builds on that proposed by Hawley and Dymond (1988), whereby the spatial relationship between landslide scars and trees is quantified as a function of distance. Their study was limited to a single hillslope, single species, and treated as uniform in terms of slope stability in the absence of trees. Given that the properties of trees will vary in response to their environmental setting, observations over large areas are essential to infer the average tree influence. The high magnitude rainfall events between 2005 and 2010 triggered thousands of shallow landslides which span a variety of environmental gradients and will increase the likelihood for patterns to emerge from observations at landscape scale.

For each class (j) of the four dominant tree species classes, the tree influence model M_j is developed as a function of soil surface eroded by landsliding $f(r)$, as follows: we denote the distance from the nearest tree as r and $b = f(r)$ is the fraction of soil eroded (Fig. 5). We will examine the relationship between b and r, whereby the effect of the trees is expected to decrease with increasing r until $f(r)$ approaches an asymptote $b = constant$ at a larger r. This asymptotic value of b is denoted by b_c and the value of r where $b = constant$ denotes the radius of the maximum distance of influence of the "average" tree, r_{max}. Note, all reference to eroded soil surface in this analysis is planar in nature, not volumetric.

Here, we specifically wish to isolate the influence of individual trees on slope stability in pastoral hill country, which we define using land cover classes from the NZ Land Cover Database of New Zealand (LCDB v4.1[1]) and a slope threshold. LCDB is a manually-mapped land cover classification with a minimum area unit of 1 ha, which means most silvopastoral landscapes are classified as 'Grasslands' (85.4% of study area) or depending on the density of trees, as one of the following classes: 'Broadleaved Indigenous Hardwoods' (1.1%), 'Deciduous Hardwoods' (1.3%), 'Gorse and/or Broom' (0.3%), 'Mānuka and/or Kānuka' (3.9%). Exotic forests (3.8%), indigenous forests (0.9%), and 'Short-rotation cropland' (2.6%) were removed. In addition, trees were excluded if located on slopes where landsliding was unlikely to occur, defined as slopes below the 1st percentile in the slope density distribution of the landslide inventory, which is 17.5° (Fig. 6). Thus, 92.3% of the study area is classified as a land cover typical of pastoral hill country, and 52.0% of the study area exceeds the threshold of 17.5°, resulting in a slope-pasture mask of 377.8 km^2. Therefore, according to this simplified definition, 44.8% of the study area is pastoral hill country. To isolate the influence of a single tree at a given pixel, areas of potential co-influence are removed by creating 15-m buffers around tree points and removing intersecting areas (Fig. 5). A 15-m radius centred on a tree point, and its vertical below-ground extension, is a conservative estimate of the ground area likely to contain most roots and affect slope stability (e.g. Douglas et al. (2013) used a 10-m radius). Tree points represent the centroid of delineated tree crowns generated by pycrown, hereafter referred to as treetops. Further, a 15-m buffer is drawn around all trees not belonging to species class j in an iterative process to create a species-specific mask to treat each class independently (Fig. 5).

Two final steps were involved in the calculation of the empirical tree influence models on slope stability (TIMSS) for each of the four species classes. A raster was generated using a euclidean distance algorithm, representing the distance to the rasterized treetops at 1 m GSD. Landslide scars were merged using unique distance codes, resulting in a raster with values indicating distance from treetop and presence/absence of landslide scars. The fraction of soil surface eroded as a function of distance from tree could then be calculated for each tree species using the number of spaced trees within the slope-pasture mask and landslide

---

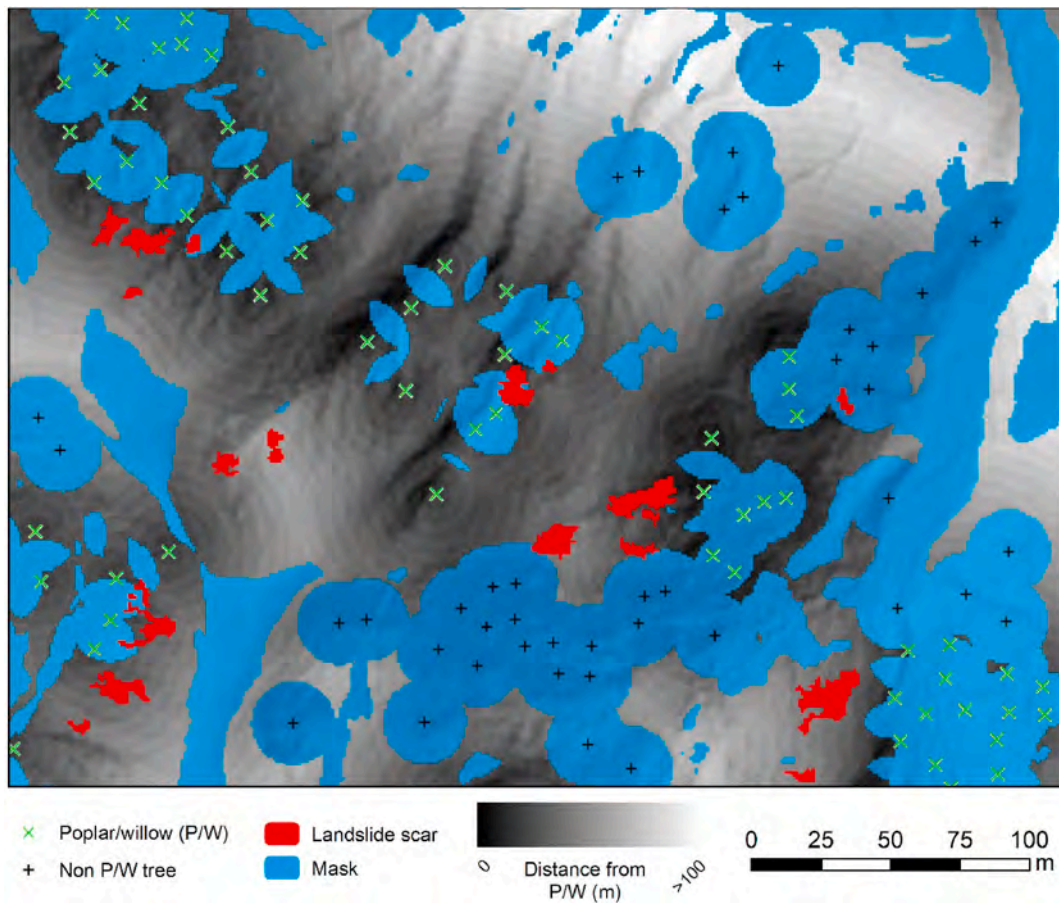[1] https://doi.org/10.7931/L17H3.

Fig. 5. Illustration of method used to determine the influence of individual trees on slope stability as a function of distance (r) – here for the poplar/willow (P/W) class: The fraction of soil eroded is calculated at 1-m intervals from P/W trees. To isolate the effect of individual P/W trees, a mask is used to remove 1) 15-m buffers around all non-PW trees, 2) intersecting 15 m buffers of P/W trees, and 3) slopes less than 17.5°.

scars (Table 5).

A nonlinear least-squares logistic regression model was used to fit $f(r)$ for each of the four species classes (Bates and Watts, 1988). The $f(r)$ curves are sigmoidal in shape, which has been found in other root distribution models, e.g. in relation to root density (Sakals and Sidle 2004) and root reinforcement (Schwarz et al., 2012). The logistic growth function is defined as:

$$f(r) = \frac{b_c}{1 + e^{\frac{xmid-r}{scal}}} \tag{1}$$

where b_c is a parameter representing the asymptote; *xmid* is a parameter representing the r value at the inflection point of the curve; and *scal* a scale parameter on the input axis.

The Selfstart function SSlogis in R first evaluates the logistic function and its gradient, then creates initial estimates of the parameters b_c, *xmid*, and *scal*, which are fed to the nonlinear function to find the best-fit logistic equation. Goodness of fit was calculated using R-squared, and 95% confidence and prediction intervals were calculated for each model. The maximum effective distance r_{max} is defined as the point where $r = .95b_c$.

Thus, for each species class j, the TIMMS (M_j) are defined as the reduction in soil surface eroded, expressed as:

$$M_j = b_c - f(r) \tag{2}$$

Inserting $f(r)$ from equation (1), and following normalization to 0–1, M_j is quantified as:

$$M_j = 1 - \frac{1}{1 + e^{\frac{xmid-r}{scal}}} \tag{3}$$

where M_j is the species-specific mitigation at a given pixel for an individual tree. When applied spatially, the influence of more than one tree is assumed to be additive, whereby the upper bound of trees contributing to slope stability at a given pixel is assumed to be 4. The TIMSS are thus a 2-dimensional representation of biophysical erosion and sediment control at 1 m GSD.

3. Results

3.1. Landslide inventory

The final landslide dataset consists of 43,069 landslide scars that were triggered by the 2005 and later storm events (Fig. 7). Median scar area is 49 m^2, mean 82.1 m^2, which is consistent with findings of previous studies (De Rose, 2012; Betts et al., 2017; Smith et al., 2021). The bands of limestone within the study area are notably absent of landslide scars (Figs. 1 and 7). The highest density of scars is found in the southern part of the study area, where high-magnitude rainfall events in 2005, 2006 and 2009 (72 h totals of 197–283 mm) coincided with the steep and highly susceptible terrain, underlain by mudstone and fine siltstone. Mean slope of landslide scars is 32.2°, with a standard deviation of 5.1° (Fig. 6).
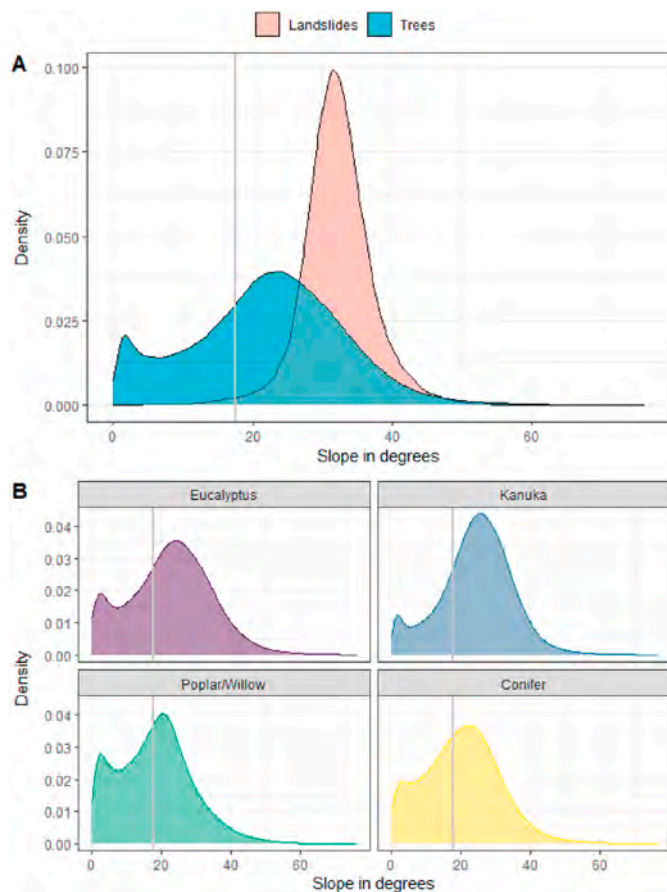
Fig. 6. A: Density plots of shallow landslide scar slopes and slopes where trees are located on pasture. B: Density plots of slopes according to species class within pasture mask. The vertical line represents the 1st percentile (17.5°) of landslide slopes, which is the cut-off used for tree selection.

3.2. Rural tree species classification

The results of the SVM rural tree species classification are dependent on the performance of both ITC delineation using pycrown and the species classification using SVM and selected set of predictors (Table 2). In dense stands of kānuka and coniferous species, the number of trees was consistently underestimated (Table 3). This is partially explained by reasonably smooth canopies in areas of dense kānuka. Reducing the window size to a 3-m radius resulted in a slight improvement in the kānuka (0.39 of field counts; compare Table 3) and conifer (0.47) classes but led to an overestimation in the eucalyptus (1.07) and poplar/willow (1.15) classes.

In terms of performance of predictors, variable selection for the tree classification was informed by the pair-wise ROC curves and calculation of the AUC scores. Tree height (TH) was the sole variable to score consistently less than 0.6 across all species classes (Fig. 8). Removal of *TH* resulted in a marginal improvement of the model (0.1%) and confirms TH as a poor predictor (Table 4). The Kappa score also increased from 0.8879 to 0.8895. The next lowest AUROC score was the SD of NDVI from 2013 imagery (ndvi_13_sd). However, removal of *ndvi_13_sd* led to a reduction in mean accuracy. The ranking of variables using AUROC across classes shows there is no further variable that is clearly under-performing and potentially reducing the predictive power of the model. However, a correlation matrix of all variables found a strong correlation (−0.91) between mean brightness (2013) and mean NDVI (2013). Yet, removal of mean brightness (2013) resulted in a significant reduction of accuracy, and therefore contributes to the performance of the classifier in interaction with mean NDVI (2013). Therefore, the final

SVM model includes 11 predictors following removal of *TH* (Table 4), and trained on 9260 tree crowns from sites 1 and 2. A final accuracy of 92.6% and a Kappa value of 0.89 proves the SVM model to be an excellent classifier for these tree species classes.

Table 5 presents the results of the classification. Trees that fall outside the pasture mask are either forestry blocks, areas of scrub, or indigenous vegetation. Thus, the dominant species in areas of pasture (776 km^2) is kānuka (373,000 trees), followed by poplar and willow species (207,000). When considering the underestimation of pycrown for the kānuka and conifer species, the corrected number is likely to be approximately 1.07 million kānuka, and 111,000 conifer stems. Interestingly, a large proportion of kānuka (76.4%) are located on steep slopes (>17.5°), where landslide erosion is more likely (Fig. 6). Since kānuka is often found alongside mānuka, and difficult to distinguish spectrally, the classified kānuka in the study area includes mānuka. A lesser proportion of poplar and willows (52.9%) and eucalyptus trees (66.9% of the 60,500) are found in the same slope category.

3.3. Empirical tree influence models on slope stability

Table 5 lists the number of trees used to develop the TIMSS for each of the four species groups. According to the results of the classification, kānuka is the most dominant species in pastoral hill country (slopes >17.5°) in the study area, making up 62% of all trees, or 79% using the correction factor. Of the 262,000 poplars and willows, 109,000 are within the pasture-slope mask, of which 25,000 are spaced at a minimum of 15 m and were used to isolate the influence of an individual poplar/willow on slope stability. Since most conifers (*Pinus radiata*) are found in forestry blocks or shelter belts located on farms within the study area, merely 1% of all pines and 7% of eucalyptus are located as space-planted trees on slopes in areas of pasture. This underscores the need for a large study area to successfully use the inferential method, since different species are planted at different densities and locations depending on their purpose.

The results of $f(r)$ and M_j for the four species classes are shown in Figs. 9 and 10, respectively. The points in Fig. 9 are the measured mean values of fractions of eroded soil at each 1 m increment away from the trees. The four non-linear models were then used to predict the maximum distance of influence and are plotted in Fig. 9, as follows: A) poplar/willow 20 m; B) kānuka 17 m; C) conifer 17 m; and D) eucalyptus 13 m. The asymptotic value b_c is different for each of the four species groups, which reflects the local environment in which the trees selected for the analysis are predominantly located. Based on Fig. 9, eucalyptus, poplars, and willows are situated on slopes with higher rates of erosion than kānuka and coniferous species, and consequently have larger asymptotic values.

Fig. 10 shows the results of the normalized reduction in eroded soil $b_c − f(r)$, i.e. M_j. Where the layout of trees is such that more than one tree contributes to slope stability at a given location, the influence on slope stability is assumed to be additive. Therefore, TIMSS values can exceed 1 when applied spatially (Fig. 12). Eucalyptus trees have the greatest mean influence between 0 and 5 m from trees, but the least reach, with a maximum effective distance of 13 m. Poplars and willows have the greatest maximum effective distance of 20 m, and the tree influence decreases more slowly with increasing r compared to the other three curves. The influence on slope stability of the conifer class decreases rapidly with increasing r, reaching a value of 0.3 at 9 m, and a maximum effective distance of 17 m. Kānuka has the same maximum effective distance as conifers, yet reaches an TIMSS value of 0.3 at 10 m. In total, 43.8% of the area (165.3 km^2) comprising pastoral hill country in the study area has increased slope stability due to the presence of trees, i.e. an TIMSS value greater than 0. The remaining 56.2% of pastoral hill country (212.5 km^2) are untreated slopes that are susceptible to landslide erosion.
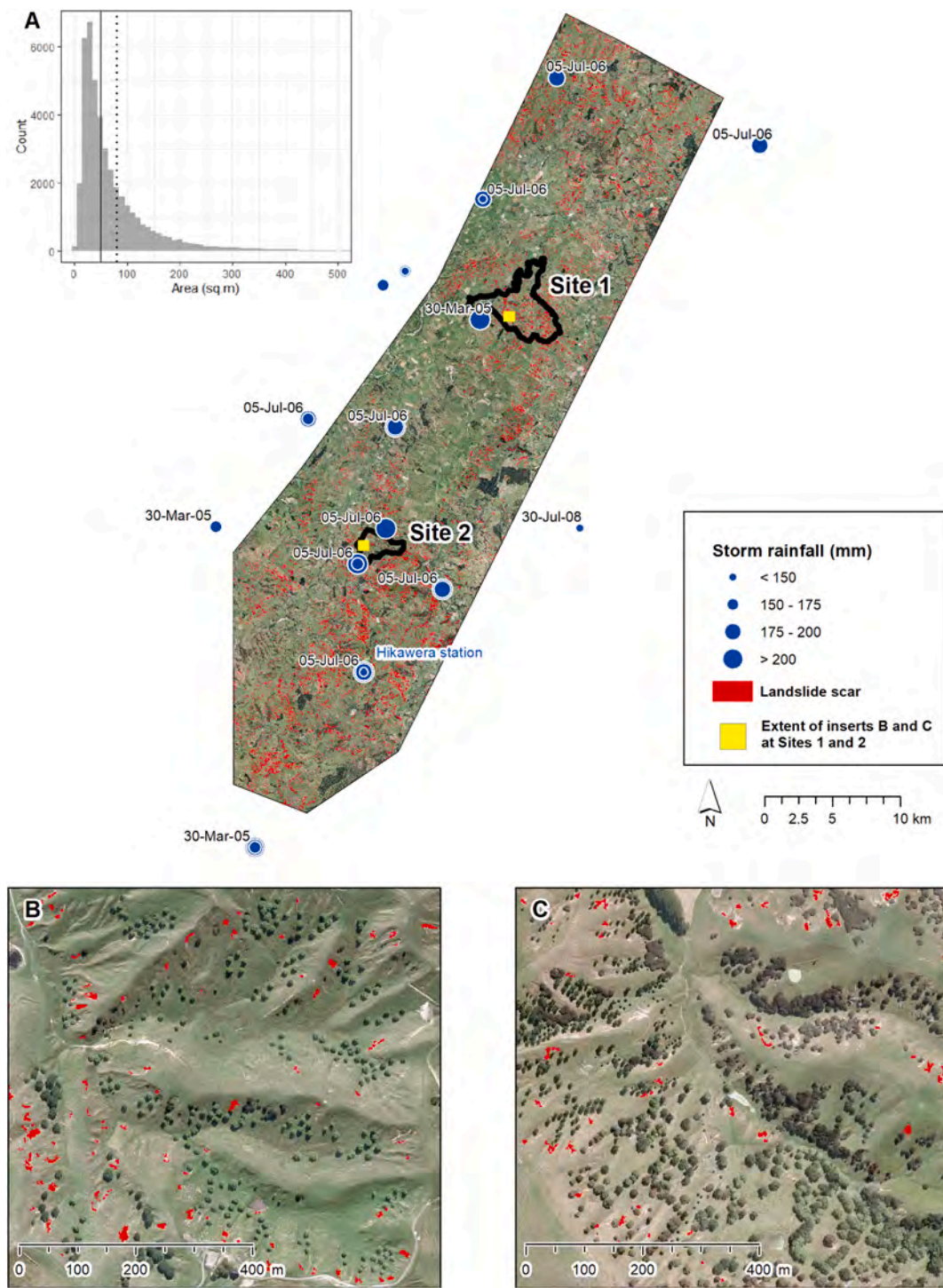
Fig. 7. Distribution of storm-triggered landslides (red polygons) mapped in this study, and the rainfall magnitude of storms > 120 mm for the period March 2005 to January 2010. The beginning date of the events which recorded the highest rainfall during this period are labelled at each rain gauge. The extent of farms (sites 1 and 2) used for tree species field mapping is also shown. Insert A: Distribution of landslide scar size (m²), including vertical lines of median (49 m²) and mean (81.1 m²); Insert B is the extent of yellow frame at Site 1; Insert C is the extent of yellow frame at Site 2. (For interpretation of the references to colour in this figure legend, the reader is referred to the Web version of this article.)

4. Discussion

4.1. Rural tree species classification

Inclusion of both mean and SD brightness/NDVI were shown to be good predictors and enhanced the discrimination between species classes. Yet, tree height was found to be a poor predictor of species. This

can be explained by the significant variation within species classes and similar mean tree heights across classes, which is likely due to a range of tree ages (Fig. 11). The overall accuracy of 92.6% using k-fold cross-validation with the entire dataset of 9,260 tree crowns is a good measure of expected accuracy achievable in the wider study area. Yet, according to the data obtained in the field, approximately 10% of mapped trees in the study area do not fit into the four dominant species classes

Table 3

Pycrown calibration results, and parameters used: Window size (ws); Hmin – threshold below which a pixel cannot be a tree; th_seed – Growing threshold 1; th_crown – Growing threshold 2; Maximum crown value of the crown diameter.

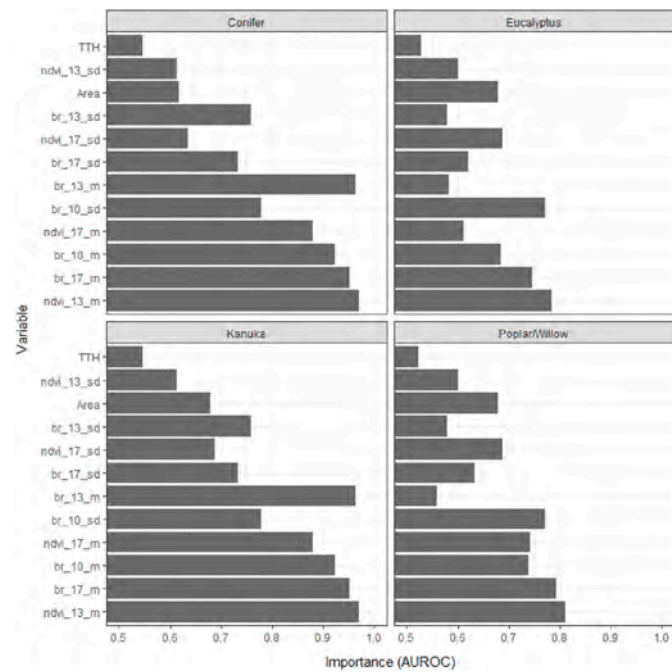| Species class	Field count	pycrown count	Proportion of field count
Conifer	693	238	0.34
Kānuka	278	97	0.35
Eucalyptus	341	329	0.96
Poplar/willow	1179	1174	1.00
Other	239	97	0.41
Total	2491	1838	0.74
pycrown parameters:	ws 5, Hmin 1.5, th_seed 0.45, th_crown 0.55, max_crown 8		

Fig. 8. Variable importance using AUROC for selection of best predictors. An AUC of 1 would indicate perfect classification, while an AUC score of 0.5 equates to performance no better than a random guess. See Table 2 for interpretation of abbreviated variable names.

Table 4

Classification accuracy following 5x 10-fold cross-validation ($\sigma = 0.05$, cost penalty = 10) with different input variables. Accuracy of the final model was improved following extensively tuned (best model: $\sigma = 0.05$, cost penalty = 15)

					Final model
Tree Height (m)					
Tree crown area (m2)					
Mean brightness 2010					
Standard deviation brightness 2010					
Mean brightness 2013					
Standard deviation brightness 2013					
Mean NDVI 2013					
Standard deviation NDVI 2013					
Mean brightness 2017					
Standard deviation brightness 2017					
Mean NDVI 2017					
Standard deviation NDVI 2017					
Accuracy (%)	92.40	92.51	92.05	89.83	92.58
Cohen's Kappa	0.8879	0.8895	0.8828	0.8496	0.8905

Table 5

Tree selection for tree influence models.

	Eucalyptus	Kānuka	Poplar/ willow	Conifer	Total
Total number of trees in study area	77,920	405,649	261,656	118,631	863,856
Number of trees in pastoral land	60,524	372,579	206,773	37,614	677,490
Number of trees in pastoral hill country	40,508	285,251	109,015	22,307	457,081
Number of trees spaced >15 m	5476	53,974	25,006	1429	85,885
Trees selected of total (%)	7%	13%	10%	1%	10%
Area of species-specific mask (km^2)	243.7	279.5	266.1	252.1	–

the model, further training samples from additional classes are needed.

This is the first attempt at tree species classification of ITCs at landscape scale in New Zealand. In their review on tree species classification, Fassnacht et al. (2016) acknowledge the significant challenge of developing classifications over large geographic extents. Field counts of stems showed that LiDAR based delineation of individual tree crowns with pycrown (Zörner et al., 2018) produced very accurate results for space-planted poplar, willow, and eucalyptus trees. However, since kānuka is most often found in relatively dense stands with little variability in tree heights, we counted an average of 2.86 stems in the field for every pycrown-delineated tree crown. Coniferous species are often planted as shelterbelts, or as relatively small, densely planted blocks (e. g. 2 ha). Their close spacings present a similar difficulty for accurate tree crown delineation, with an average of 2.94 stems per delineated tree crown. To improve discrimination of individual kānuka crowns, increasing the resolution of the LiDAR DEMs (e.g. 0.5 GSD) may help. While this would improve the gradient between trees, it can also result in an overestimation of tree crowns, as subcomponents of crowns such as individual branches, can be delineated as separate objects. Recent advances have been made using machine learning to integrated crown delineation from LiDAR with optical imagery and provide a highly adaptable means for accurate delineation across multiple forest types (Weinstein et al., 2019, 2020a, 2020b). However, on pastoral land, conifers only make up a small proportion of all trees (111,000 ± 16.7%), or 1.4/ha. As to be expected, eucalyptus is the least common species class, accounting for only 4% of trees in pastoral land in the study area. Poplar and willow species amount to 14%, and 11% on hillslopes, making up 109,000 trees in pastoral hill country, which amounts to an average of 3.2 sph. Poplars and willows are therefore the most abundant exotic species (51% of exotics) that have been intentionally planted for erosion and sediment control.

A somewhat unexpected finding is the dominance of kānuka in the study area, which consists of original bush remnants and natural regenerated trees. Kānuka makes up 79% of trees in pastoral hill country in the study area, averaging 24.1 sph following correction (Table 6). However, only 19% of these kānuka are spaced more than 15 m apart (Table 5), so the majority are growing in dense patches, which promotes slope stability, but likely reduces pasture productivity. Kānuka are successional species and are among the first to colonise marginal land, including eroded hillslopes (Smale et al., 1997). Indeed, 76.6% of the kānuka on pastoral land are on susceptible hillslopes (>17.5°) – which is a large proportion compared to 52.7% of poplars and willows on pastoral land (Table 6; Fig. 6). Despite being abundant in pastoral hill country, research on the impacts of kānuka on landslide erosion are limited (Watson et al., 1995, 1999; Ekanayake et al., 1997) and mostly have high density stands of naturally reverting kānuka and mānuka as the object of their investigation – as opposed to widely spaced,
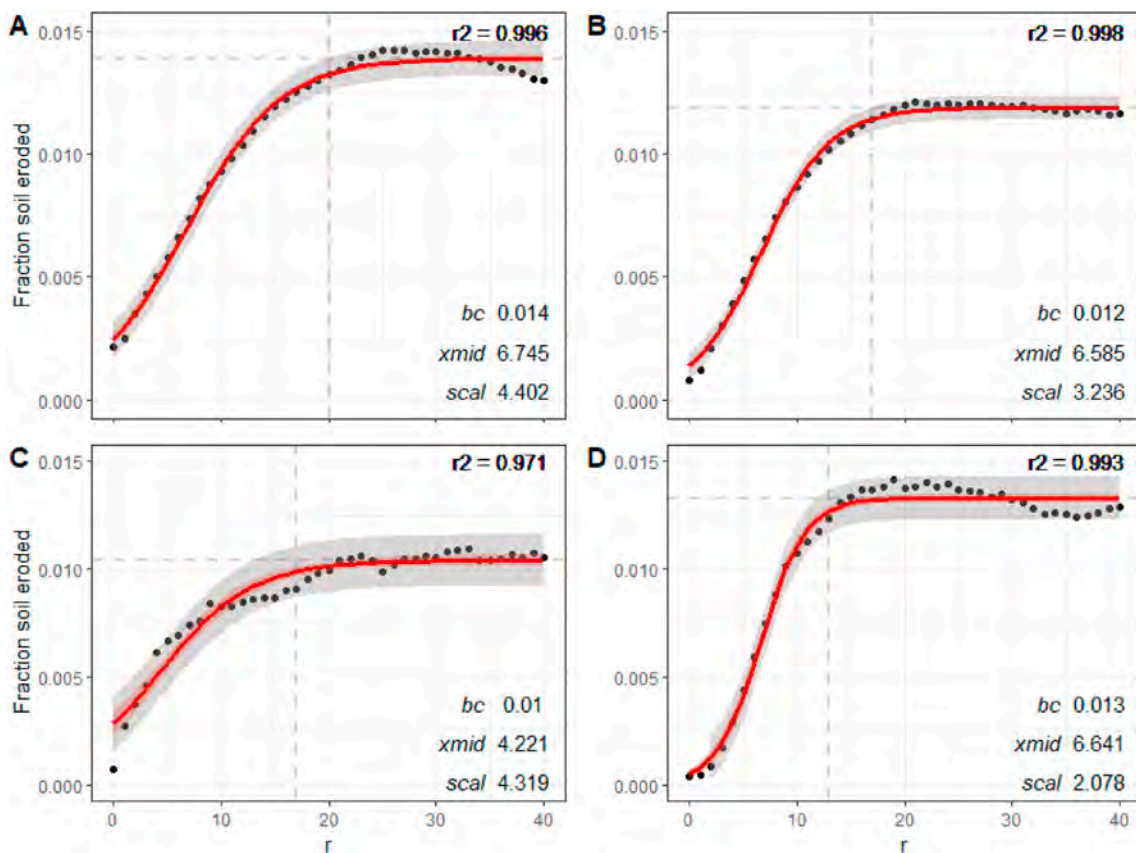
used here (Table 1). Accounting for this source of error, the overall classification accuracy is likely to be 83.3% since predictions can only be made with the classes available to the SVM classifier. To further improve

Fig. 9. For the four species classes A) poplar/willow, B) kānuka, C) conifer, and D) eucalyptus: Mean fraction of eroded soil $f(r)$ at distance (m) from tree, fitted using non-linear logistic model SSlogis with 95% confidence (red) and prediction (grey) bands. (For interpretation of the references to colour in this figure legend, the reader is referred to the Web version of this article.)
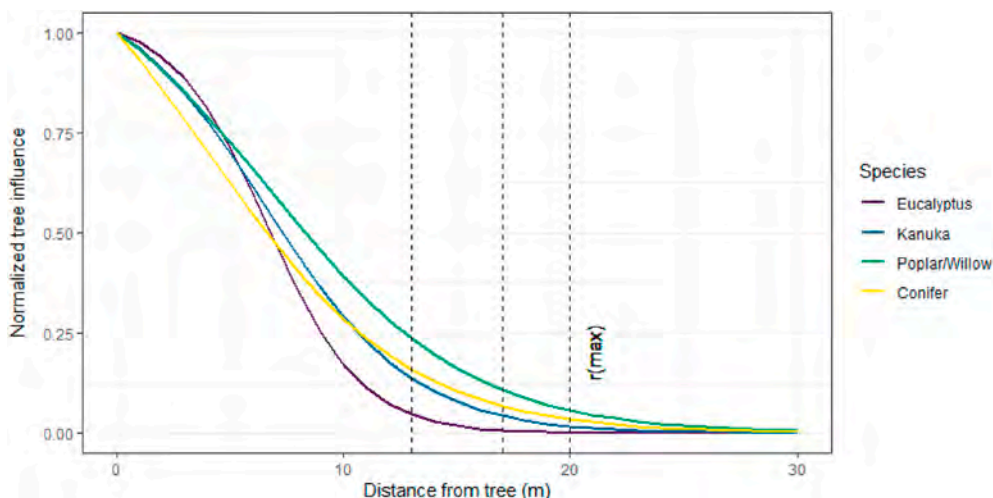

Fig. 10. For the four species classes conifer, eucalyptus, kānuka and poplar/willow: Normalized mean tree influence M_j (0–1) for an individual tree, as reduction in eroded soil $b_c - f(r)$. Vertical lines show the maximum effective distance of 13 (Eucalyptus), 17 (conifer, kānuka) and 20 (poplar/willows) meters.

low-density kānuka.

Investigating landslide densities in reverting kānuka and mānuka, Bergin et al. (1995) found landslide damage to 10-year-old stands was estimated to be 65% less than that sustained by pasture and 90% less in 20-year-old stands, and almost 100% in still older stands. They also found a relationship between stem density and age, with young stands of <10 years age typically containing 20,000 sph and older stands (30–40-year age class) 3000 sph. Bergin et al. (1995) further note that

under-stocked stands gave a reduction in landsliding comparable with fully stocked stands of similar age. This indicates that thinning kānuka stands on hillslopes may be a reasonable erosion mitigation strategy to both increase pasture productivity while maintaining increased levels of slope stability. Furthermore, these findings challenge the common perception of kānuka as a weed and the related scrub-clearing method aimed at increasing pasture productivity (Allen et al., 1992). In commenting on the practice of kānuka clearance, Norton et al. (2020)
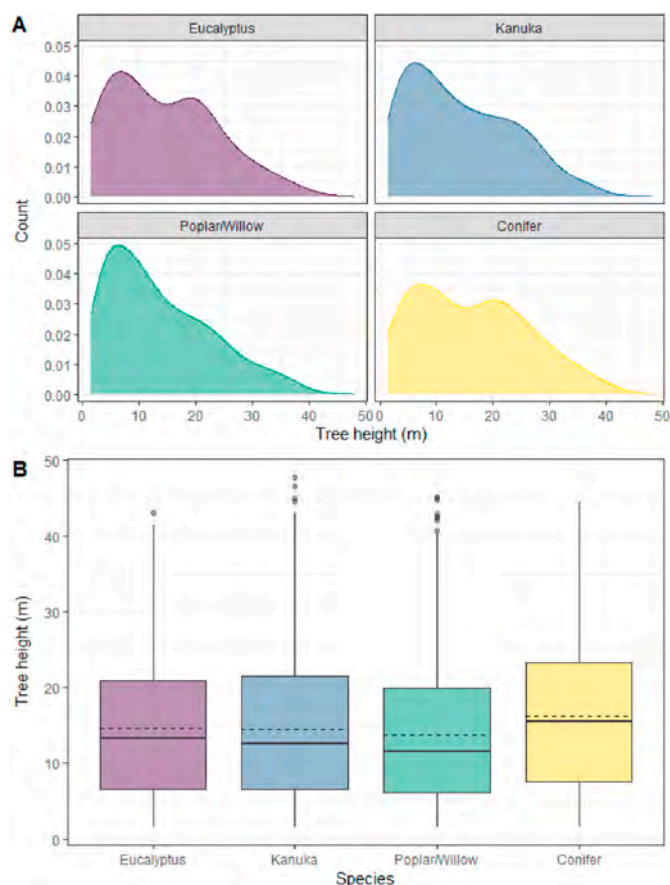
Fig. 11. For the four species classes at Sites 1 and 2 combined: A) Density plots and B) boxplots of tree heights with median (solid line) and mean (dashed line) shown.

suggest landowners need to be better incentivised to promote land management practises that retain and enhance biodiversity outcomes. Results of this study can inform the densities required to achieve added slope stability, which is discussed in the following section.

4.2. Interpretation of empirical tree influence models

Further developing a method first introduced by Hawley and Dymond (1988), we have demonstrated an alternate approach to existing physical root distribution models aimed at generating a tree influence layer for the dominant species found in New Zealand's pastoral hill country (Fig. 12). Such layers can subsequently be incorporated into landslide susceptibility analyses to quantify the species-specific reduction in probability of landsliding achieved due to the presence of space-planted trees and pre-existing woody vegetation such as kānuka. Thus, we aim to fill the gap in scale between physical models that quantify root reinforcement for homogenous tree stands, and landslide susceptibility modelling at regional scale that commonly uses land cover data as a proxy for the effect of the hydrological and mechanical influences of woody vegetation. It is important to note that the normalized TIMSS are a relative measure of individual tree influence on slope stability and, besides the distribution of the curves, are not directly comparable. For a given location, a value of 1.0 for the poplar and willow TIMSS will equate to a greater increase in soil shear strength than a value of 1.0 in the conifer TIMSS since the magnitude of increase in root reinforcement differs due to variations in the tensile strengths of root fibres and resulting soil-root frictional interactions (Schmidt et al., 2001; Schwarz et al., 2010a,b).

Future research is needed to quantify differences in the magnitude of

TIMSS by: i) calibration using published datasets of tensile strength measurements, such as the mean live-root wood tensile strengths of common indigenous, plantation and scrub species by Watson and Marden (2004); or ii) landslide susceptibility assessments, which can quantify the relative contribution of the four different TIMSS as a reduction in the probability of landslide occurrence. Additionally, the TIMSS have potential to be further split by tree height as a proxy for age (Fig. 11), since the influence of trees on slope stability increases with above- and below-ground biomass growth. If successful, this would allow the tree influence on slope stability to be predicted based on allometric variables for each species class, which would provide a more nuanced representation of added soil shear strength due to trees.

The discussion thus focuses on the shape and maximum distance of the TIMSS curves (Fig. 10). Root distribution data from extractions and/ or models are limited for comparison purposes. Yet, we found very similar relationships expressed in the TIMSS to existing root distribution models for similar species (Abernethy and Rutherfurd, 2001; Sakals and Sidle, 2004; Schwarz et al., 2012, 2016). The model developed by Sakals and Sidle (2004) to assess the spatial variability of root cohesion based on a calibration of measured root cohesion from a Douglas-fir stand of 20 root systems found the relationship between normalized root densities and root influence radii to be sigmoidal in shape, differing slightly between two age groups of trees. This suggests the TIMSS have potential transferability to other species and environmental settings, where the representation of individual trees for landslide susceptibility modelling is desired, e.g. in agroforestry landscapes (van Noordwijk et al., 2019; Hairiah et al., 2020).

A further comparison can be made to the root-bundle model calibrated by Schwarz et al. (2016) using two root distribution datasets of fully excavated poplars from Gisborne and samples from 20 trenches at a site near Palmerston North, New Zealand, planted in a range of high densities (89–237 sph) according to a Nelder planting design (Phillips et al., 2014). The results were used in slope stability calculations to quantitatively evaluate the mechanical stabilization effects of spaced trees on pastoral hill country. The maximum lateral root spread was reported as 13.3 m for 2-year-old poplar species in the Gisborne site, and estimated as only 4.2 m for the high-density stands at the Palmerston North site. The modelled spatial root reinforcement curve in the root-bundle model used a Weibull survival function, which is similar to the non-linear logistic regressions fitted for the TIMSS. However, it is clear there are significant differences between the maximum effective distance of poplars/willows modelled by Schwarz et al. (2016) and that observed in the TIMSS, which can be explained by considering: i) the influence of different environmental conditions as demonstrated by lateral root growth of 1–2-year-old trees at the flat, irrigated site with free draining alluvial soils exceeding that of the 10-year-old trees on 5–20° slopes at the Palmerston North site with silt-loam soils featuring various mottles and concretions in the sub-soil; ii) different tree densities and sampling methods (full excavations versus trenches), may have also contributed to the large difference found between their two sites; iii) the hydrological influence was not quantified by Schwarz et al. (2016), which may partly explain the differences from the maximum distance observed in the TIMSS; and iv) the average age of poplars and willows in our study area in the Wairarapa will likely exceed the age of trees for which root data is available for comparison purposes (e.g. McIvor et al., 2008; 2009; Schwarz et al., 2016).

Most of the poplar and willow trees mapped at Sites 1 and 2 were planted in the 1980s to early 2000s, with a mean tree height of 13.7 m (Fig. 11). While there are no published data of root densities of fully mature, widely-spaced trees, a comparison with the largest dataset of full excavations of poplars, documented by McIvor et al. (2008, 2009), can further help with an interpretation of the TIMSS. Based on their observations of 'Veronese' poplar clones aged between 5 and 12 years, they found maximum lateral root distance extended up to 14 m. At 14 m, the poplar and willow TIMSS is 0.2. The remaining difference in $f(r)$ where $14 < r < 21$ may be attributable to both the younger age of
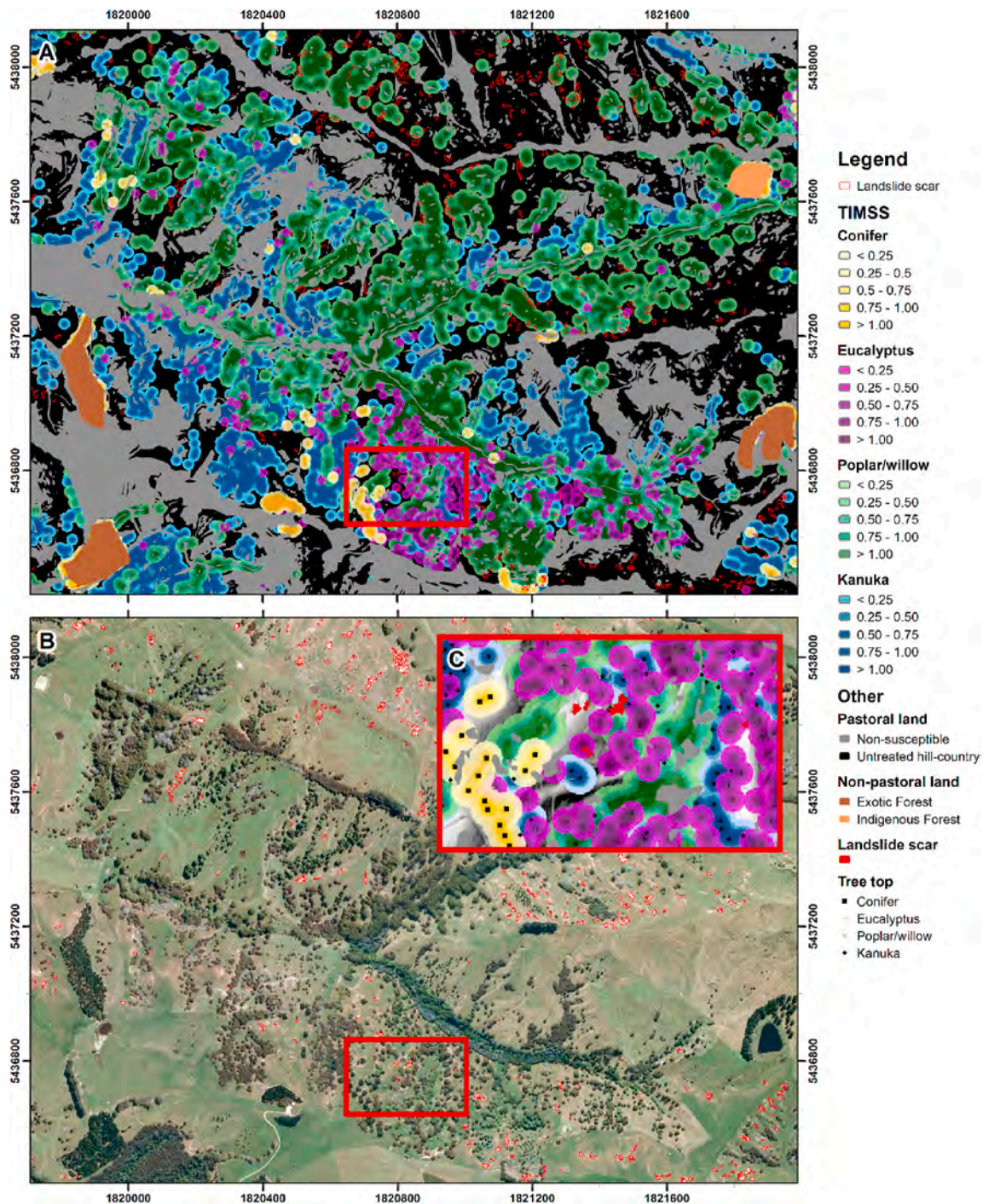
Fig. 12. A: For an area at Site 2, empirical tree influence models on stability for the four species classes: conifer, eucalyptus, poplar/willow and kānuka, non-susceptible pastoral land (defined by slope threshold of 17.5°), and untreated pastoral hill country; B: Regional multispectral orthophotos (2010) showing land-slide scars mapped in imagery. Red frames in A and B show extent of Insert C: Illustration of landslide causation: though trees contribute to slope stability, they do not always prevent landslide erosion – a reflection of a multivariate problem. Note, the influence of more than 1 tree at a given location is assumed to be additive, which is why values exceed 1. Map projection is New Zealand Transverse Mercator (NZTM). (For interpretation of the references to colour in this figure legend, the reader is referred to the Web version of this article.)

excavated trees by McIvor et al. (2009) and the hydrological influence of trees that modifies water infiltration and soil moisture content (Phillips and Marden, 2005; Zillgens et al., 2007; Stokes et al., 2009; Gonzalez-Ollauri and Mickovski, 2017). Even though these excavations were undertaken for young trees, they do support the observation that mature poplars and willow trees have a maximum effective distance on slope stability of about 20 m. Further experimental research and root data collection of fully mature poplar and willow trees are required to

confirm the findings of this study. However, as was found by Schwarz et al. (2016), the challenge associated with measurements taken from excavations is the high variability in root distributions within single species due to varying environmental constraints. McIvor et al. (2009) found soil depth and associated water storage capacity to be likely limiting factors for growth and root development. There were also indications that terrain morphology influenced the root morphology with roots extending further uphill on steeper slopes.

Table 6

Corrected tree counts and mean densities in pastoral land and in pastoral hill country in study area. The combined error tree species classification and absent species classes is ±16.7%. Pastoral hill country is defined using a slope threshold of 17.5°.

Corrected tree counts	Eucalyptus	Kānuka	Poplar/ willow	Conifer	Total
Number of trees in pastoral land (sph)	60,524 (0.8)	1,064,511 (13.7)	206,773 (2.7)	110,629 (1.4)	1,442,438 (18.6)
Number trees in pastoral hill country (sph)	40,508 (1.2)	815,003 (24.1)	109,015 (3.2)	65,609 (1.9)	1,030,135 (30.8)
Trees in pastoral land (%)	4%	74%	14%	8%	100%
Trees in pastoral hill country (%)	4%	79%	11%	6%	100%

Excavations of mature kānuka trees by Watson et al. (1995) found a mean maximum root length of 3.6 m and a maximum root length of 6.1 m for the 32-year-old age group. Adopting a correction factor of 0.35 delineated crowns per stem, the kānuka TIMSS can be interpreted accordingly (Table 3). Thus, the maximum effective distance of 17 m is due to the influence of approximately 3 stems, and the kānuka in the study area are largely mature trees that are several decades old so will likely have more developed root systems than that documented by Watson et al. (1995). The same study also excavated three *Pinus radiata* aged 25 years and found a mean maximum root length of 9.1 m. Once more, adopting a correction factor of 0.34, the conifer TIMSS with a maximum effective distance of 17 m can be interpreted as the effect of approximately 3 stems. A further important consideration is that the tensile strength of fine roots differs across species classes, and is a limiting factor for *Pinus radiata*, whose mean live-root tensile strengths are only 40% and 50% of kānuka and 'Veronese' poplar (*Populus deltoides x nigra*) root strengths, respectively (Watson and Marden, 2004).

However, in the absence of comparable data, the maximum distance of influence presents some initial interpretational difficulty; and yet, the data presented here are based on empirical observations of the spatial relationship between trees and landslide erosion. Several factors need to be considered when interpreting the results such as the respective contributions of the hydrological and mechanical processes by which vegetation modifies slope stability. The TIMSS represent the mean spatial distribution of the combined mechanical and hydrological influence imparted on the soil during the rainfall events that triggered the landslides between 2005 and 2010. More detailed analysis of antecedent soil moisture conditions leading up to the storms of 2005, 2006, and 2009 may shed light on the respective roles of mechanical and hydrological processes of trees, particularly given that, with the exception of the March 2005 storm, the remainder were during the winter month of July where interception and evapotranspiration are less relevant due to leaf fall. Yet, despite being the only deciduous species class, the poplar-willow TIMSS outperforms the other three classes in terms of the magnitude of influence beyond 4 m, which supports the fact that the mechanical mechanism of poplar and willow species is significant due to the high tensile strengths of the roots.

4.3. Implications for land management in pastoral hill country

There has been strong emphasis on biological erosion control in New Zealand's pastoral hill country – either through space-planted trees or blanket afforestation, because of its relative low cost and its effectiveness (Phillips and Marden, 2005; Douglas et al., 2013). In more recent times, erosion mitigation has been made a component of Farm Environment Plans (FEP), which are comprehensive plans undertaken by regional councils, farmers or other industry groups that integrate soil conservation into land management practices and farming operations (Phillips et al., 2000, 2008; Manderson et al., 2007; Basher, 2013; Basher et al., 2008, 2016a, b; Douglas et al., 2008; Mackay et al., 2012; Collins et al., 2014). Yet, little is known about the effectiveness of individual trees and stands and the overall effectiveness of these measures at landscape scales. Both the rural SVM tree species classification produced for New Zealand's pastoral hill country and the derived TIMSS can be applied at farm to landscape scales to inform on which species are either pre-existing in the landscape or have been successfully established in the context of FEPs (Fig. 12). Furthermore, through integration into high-resolution landslide susceptibility modelling, it is now possible to both i) quantify the mitigation effectiveness of individual trees and compare species and ii) inform on where to prioritize future mitigation, given the spatial probability of landslide occurrence, which can be modified by the presence or absence of trees. Mitigation effectiveness is a multivariate problem, as it is dependent on site-specific conditions, which vary with, for example, slope gradient, soil, and rock type. Therefore, including the four TIMSS as covariates within a landslide susceptibility assessment can provide a statistical measure for the respective contributions of each layer to slope stability. Furthermore, allometric functions could also be used to scale the TIMSS, e.g. according to tree height or area of tree canopy.

The tree densities listed in Table 6 provide an initial indication of how widely soil conservation practices have been adopted in the study area, and the spatially explicit representation of added slope stability due to trees provides further detail (Fig. 12). An average of 3.2 poplar and willow trees/ha (total of 109,000 trees), 1.2 eucalyptus/ha (41,000 trees) and 1.9 coniferous species/ha (66,000 trees) in pastoral hill country (slopes > 17.5°) reflects the work carried out by landowners and soil conservators over the past several decades. However, these numbers are also indicative of large areas of untreated land with elevated levels of landslide susceptibility. To treat the remaining 212.5 km^2 (56%) of untreated pastoral hill country (TIMSS = 0) in the study area, an additional 950,000 poplars/willows would need to be planted if using a regular grid of 15 × 15 m (44 sph), which falls within the recommended planting density of 30–60 sph (e.g. Wilkinson, 1999; Douglas et al., 2013). A planting density of 44 sph would result in TIMSS values > 0.5, which would achieve significantly more reduction in landslide erosion than values < 0.5. However, landslide susceptibility assessments incorporating the species-specific TIMSS should be used to inform on mitigation plans and planting densities in untreated terrain, since not all pastoral hill country is equally susceptible to landsliding. Variation in morphological (e.g. slope gradient; Fig. 6), geological, and hydrological geo-environmental variables can influence the potential for landslide occurrence (van Westen et al., 2008; Suzen and Kaya, 2011; Budimir et al., 2015; Reichenbach et al., 2018).

Yet, the large amount of mature kānuka in the study area, particularly on hillslopes, has reduced the propensity for landsliding in many areas (Table 6): 50% of kānuka trees growing on pastoral land are found on slopes >25°; the slope value of the 0.75 quantile is 31°. Given that the mean slope of landslide scars is 32.2° (SD = 5.1°), kānuka is the most abundant form of woody vegetation on highly susceptible slopes. Kānuka are better suited to these growing conditions than poplars and willows (Allen et al., 1992). Indeed, the 0.5 and 0.75 quantiles of slope values for poplars and willows on pastoral land are 18° and 25°, respectively, and are evidence that these unrooted poles are more likely to be planted on lower, more hospitable slopes that favour tree establishment. Thus, more planting to reinforce susceptible slopes is required to reach a recommended planting density of 25–160 sph (Hawley and Dymond, 1988; Wilkinson, 1999; Douglas et al., 2013; Schwarz et al., 2016). According to the TIMSS, poplars and willows have the greatest

influence on slope stability, but many other factors and potential co-benefits must also be considered when deciding on which species to plant (Benavides et al., 2009; Dominati et al., 2014; Kemp et al., 2018; England et al., 2020; Norton et al., 2020).

5. Conclusions

We developed a rural tree species classification of individual tree crowns using freely available high resolution multi-spectral imagery, with an overall accuracy of 92.6%. Native kānuka is the dominant woody vegetation species in pastoral hill country of the study area with an average of 24.1 sph, and thus provides a valuable soil conservation function as the most abundant species on susceptible slopes. Of exotic species that were planted for erosion and sediment control, poplars and willows make up 51% (109,000 trees) in pastoral hill country at a mean density of 3.2 trees/ha.

The novel approach demonstrated in this paper advances the method first introduced by Hawley and Dymond (1988) by developing tree influence models on slope stability (TIMSS) for four dominant tree species in New Zealand's pastoral hill country. The method uses inductive inference to infer tree influence by assessing the spatial relationship between trees and landslide erosion. This approach requires a large landslide inventory (we used >43,000 features) and many widely spaced trees (86,000) in a silvopastoral landscape. The results can both challenge and validate understanding of the role of trees on slope stability, which is typically quantified using physical root reinforcement models. The TIMSS have largely confirmed the shape and distribution of spatial root distribution models, with influence on slope stability declining rapidly with distance from trees as a sigmoid curve. Poplars and willows have the greatest maximum effective distance (20 m), and the tree influence decreases more slowly with increasing distance compared to the other three species classes. The spatial application of TIMSS has shown that 43.8% of the pastoral hill country in the study area (165.3 km^2) has increased slope stability due to the presence of trees on slopes. An additional 950,000 poplars/willows at 44 sph would be required to mitigate landslide erosion on the remaining 212.5 km^2 (56.2%) of untreated pastoral hill country in the study area. However, not all pastoral hill country is equally prone to landslide erosion. Therefore, tree influence models should be integrated into multi-variate landslide susceptibility modelling in silvopastoral and agroforestry landscapes to support the development of targeted mitigation plans.

Credit author statement

Raphael Spiekermann: Conceptualization, Data curation; Methodology, Software, Validation, Formal analysis, Investigation, Writing – original draft, Visualization. Sam McColl: Conceptualization, Supervision, Writing – review & editing. Ian Fuller: Conceptualization, Supervision, Writing – review & editing. John Dymond: Conceptualization, Supervision, Writing – review & editing. Lucy Burkitt: Conceptualization, Writing – review & editing. Hugh G. Smith: Conceptualization, Supervision, Writing – review & editing, Funding acquisition.

Declaration of competing interest

The authors declare that they have no known competing financial interests or personal relationships that could have appeared to influence the work reported in this paper.

Acknowledgements

References

Abernethy, B., Rutherfurd, I.D., 2001. The distribution and strength of riparian tree roots in relation to riverbank reinforcement. Hydrol. Process. 15, 63–79, 2001.

Allen, R.B., Partridge, T.R., Lee, W.G., 1992. Ecology of Kunzea ericoides (A. Rich.) J. Thompson (kānuka) in east Otago, New Zealand. N. Z. J. Bot. 30, 135–149.

Basher, L.R., 2013. Erosion processes and their control in New Zealand. In: JR, D. (Ed.), Ecosystem Services in New Zealand - Conditions and Trends. Manaaki Whenua Press, Lincoln, New Zealand, pp. 363–374.

Basher, L.R., Botha, N., Dodd, M.B., Douglas, G.B., Lynn, I., Marden, M., McIvor, I.R., Smith, W., 2008. Hill country erosion: a review of knowledge on erosion processes, mitigation options, social learning and their long-term effectiveness in the management of hill country erosion. In: Landcare Research Contract Report LC0708/081 for the Ministry of Agriculture and Forestry.

Basher, L., Manderson, A., McIvor, I., McKergow, L., Reid, J., 2016a. Evaluation of the effectiveness of conservation planting and farm plans: a discussion document. Landcare Research Contract Report LC2546.

Basher, L., Moores, J., McLean, G., 2016b. Scientific Basis for Erosion and Sediment Control Practices in New Zealand. Landcare Research Contract Report, p. LC2562.

Basher, L., Betts, H., Lynn, I., Marden, M., McNeill, S., Page, M., Rosser, B., 2018. A preliminary assessment of the impact of landslide, earthflow, and gully erosion on soil carbon stocks in New Zealand. Geomorphology 307, 93–106. https://doi.org/10.1016/j.geomorph.2017.10.006.

Basher, L., Spiekermann, R., Dymond, J., Herzig, A., Hayman, E., Ausseil, A., 2020. Modelling the Effect of Land Management Interventions and Climate Change on Sediment Loads in the Manawatū – Whanganui Region, p. 8330. https://doi.org/10.1080/00288330.2020.1730413.

Bates, D.M., Watts, D.G., 1988. Nonlinear Regression Analysis and its Applications. Wiley.

Benavides, R., Douglas, G.B., Osoro, K., 2009. Silvopastoralism in New Zealand: review of effects of evergreen and deciduous trees on pasture dynamics. Agrofor. Syst. 76, 327–350.

Bergin, D.R., Kimberley, M.O., Marden, M., 1995. Protective value of regenerating tea-tree stands on erosion-prone hill country, East Coast, North Island, New Zealand. N. Z. J. For. Sci. 25, 3–19.

Betts, H., Basher, L., Dymond, J., Herzig, A., Marden, M., Phillips, C., 2017. Development of a landslide component for a sediment budget model. Environ. Model. Software 92, 28–39. https://doi.org/10.1016/j.envsoft.2017.02.003.

Blaschke, T., 2010. Object based image analysis for remote sensing. ISPRS J. Photogrammetry Remote Sens. 65, 2–16.

Blaschke, T., Hay, G.J., Kelly, M., Lang, S., Hofmann, P., Addink, E., Feitosa, R.Q., van der Meer, F., van der Werff, H., van Coillie, F., Tiede, D., 2014. Geographic object-based image analysis - towards a new paradigm. ISPRS J. Photogrammetry Remote Sens. 87, 180–191.

Budimir, M.E.A., Atkinson, P.M., Lewis, H.G., 2015. A systematic review of landslide probability mapping using logistic regression. Landslides 12 (3), 419–436. https://doi.org/10.1007/s10346-014-0550-5.

Bunting, P., Lucas, R., 2006. The delineation of tree crowns in Australian mixed species forests using hyperspectral Compact Airborne Spectrographic Imager (CASI) data. Remote Sens. Environ. 101, 230–248.

Cislaghi, A., Bordoni, M., Meisina, C., Bischetti, G.B., 2017. Soil reinforcement provided by the root system of grapevines: quantification and spatial variability. Ecol. Eng. 109, 169–185. https://doi.org/10.1016/j.ecoleng.2017.04.034.

Cohen, J., 1960. A coefficient of agreement for nominal scales. Educational and psychological measurement20 (1), 37–46.

Cohen, D., Schwarz, M., 2017. Tree-root control of shallow landslides. Earth Surface Dynamics 5 (3), 451–477. https://doi.org/10.5194/esurf-5-451-2017.

Cohen, D., Schwarz, M., Or, D., 2011. An analytical fiber bundle model for pullout mechanics of root bundles. J. Geophys. Res.: Earth Surface 116 (3), 1–20. https://doi.org/10.1029/2010JF001886.

Collins, A., Mackay, A., Basher, L., Schipper, L., Carrick, S., Manderson, A., Cavanagh, J., Clothier, B., Weeks, E., Newton, P., 2014. Phase 1: looking Back. Future requirements for soil management in New Zealand. In: Prepared by National Land Resource Centre, Palmerston North for Ministry of Primary Industries.

Coppin, N.J., Richards, I.G. (Eds.), 1990. Use of Vegetation in Civil Engineering. Construction Industry Research and Infor- mation Association, Butterworths, London.

Crozier, M.J., 2005. Multiple-occurrence regional landslide events in New Zealand: hazard management issues. Landslides 2, 247–256.

Dalponte, M., Coomes, D.A., 2016. Tree-centric mapping of forest carbon density from airborne laser scanning and hyperspectral data. Methods Ecol. Evol. 7, 1236–1245.

Dalponte, M., Bruzzone, L., Gianelle, D., 2012. Tree species classification in the Southern Alps based on the fusion of very high geometrical resolution multi- spectral/hyperspectral images and LiDAR data. Remote Sens. Environ. 123, 258–270, 0.

De Jesús Arce-Mojica, T., Nehren, U., Sudmeier-Rieux, K., Miranda, P.J., Anhuf, D., 2019. Nature-based solutions (NbS) for reducing the risk of shallow landslides: where do we stand? International Journal of Disaster Risk Reduction 41 (April). https://doi.org/10.1016/j.ijdrr.2019.101293.

De Rose, R.C., 2012. Slope control on the frequency distribution of shallow landslides and associated soil properties, North Island, New Zealand. Earth Surf. Process. Landforms 38 (4), 356–371. https://doi.org/10.1002/esp.3283.

Dominati, E.J., Mackay, A., Lynch, B., Heath, N., Millner, I., 2014. An ecosystem services approach to the quantification of shallow mass movement erosion and the value of

soil conservation practices. Ecosystem Services 9, 204–215. https://doi.org/10.1016/j.ecoser.2014.06.006.

Douglas, G., Dymond, J., McIvor, I., 2008. Monitoring and Reporting of Whole Farm Plans as a Tool for Affecting Land Use Change. Report for Horizons Regional Council, Palmerston North, AgResearch.

Douglas, G.B., McIvor, I.R., Manderson, A.K., Todd, M., Braaksma, S., Gray, R.A.J., 2009. Effectiveness of space-planted trees for controlling soil slippage on pastoral hill country. In: Currie, L.D., Lindsay, C.L. (Eds.), Nutrient Management in a Rapidly Changing World. Occasional Report No. 22. Palmerston North, Fertilizer and Lime Research Centre. Massey University.

Douglas, G.B., McIvor, I.R., Manderson, A.K., Koolaard, J.P., Todd, M., Braaksma, S., Gray, R.A.J., 2013. Reducing shallow landslide occurrence in pastoral hill country using wide-spaced trees. Land Degrad. Dev. 24 (2), 103–114. https://doi.org/10.1002/ldr.1106.

Dymond, J.R., Zörner, J., Shepherd, J.D., Wiser, S.K., Pairman, D., Sabetizade, M., 2019. Mapping physiognomic types of indigenous forest using space-borne SAR, optical imagery and air-borne LiDAR. Rem. Sens. 11 (16) https://doi.org/10.3390/rs11161911.

Ekanayake, J.C., Marden, M., Watson, A.J., Rowan, D., 1997. Tree roots and slope stability: a comparison between pinus radiata and kānuka. N. Z. J. For. Sci. 27 (2), 216–233.

England, J.R., O'Grady, A.P., Fleming, A., Marais, Z., Mendham, D., 2020. Trees on farms to support natural capital: an evidence-based review for grazed dairy systems. Sci. Total Environ. 704, 135345. https://doi.org/10.1016/j.scitotenv.2019.135345.

Fassnacht, F.E., Neumann, C., Förster, M., Buddenbaum, H., Ghosh, A., Clasen, A., Joshi, P.K., Koch, B., 2014. Comparison of feature reduction algorithms for classifying tree species with hyperspectral data on three central European test sites. IEEE J. Sel. Top. in Appl. Earth Obs. Remote Sens. 7 (6), 2547–2561.

Fassnacht, F.E., Latifi, H., Stereńczak, K., Modzelewska, A., Lefsky, M., Waser, L.T., et al., 2016. Review of studies on tree species classification from remotely sensed data. Rem. Sens. Environ. 186, 64–87. https://doi.org/10.1016/j.rse.2016.08.013.

Genet, M., Stokes, A., Fourcaud, T., Norris, J.E., 2010. The influence of plant diversity on slope stability in a moist evergreen deciduous forest. Ecol. Eng. 36 (3), 265–275. https://doi.org/10.1016/j.ecoleng.2009.05.018.

Glade, T., 1998. Establishing the frequency and magnitude of landslide-triggering rainstorm events in New Zealand. Environ. Geol. 35 (August), 160–174. Retrieved from. https://link.springer.com/article/10.1007%2Fs002540050302.

Glade, T., 2003. Landslide occurrence as a response to land use change: a review of evidence from New Zealand. Catena 51 (3–4), 297–314. https://doi.org/10.1016/S0341-8162(02)00170-4.

Gonzalez-Ollauri, A., Mickovski, S.B., 2017. Hydrological effect of vegetation against rainfall-induced landslides. J. Hydrol. 549, 374–387.

Guzzetti, F., Galli, M., Reichenbach, P., Ardizzone, F., Cardinali, M., 2006. Landslide hazard assessment in the Collazzone area, Umbria, central Italy. Nat. Hazards Earth Syst. Sci. 6 (1), 115–131. https://doi.org/10.5194/nhess-6-115-2006.

Hairiah, K., Widianto, W., Suprayogo, D., Van Noordwijk, M., 2020. Tree roots anchoring and binding soil: reducing landslide risk in Indonesian agroforestry. Land 9 (8), 1–19. https://doi.org/10.3390/LAND9080256.

Hawley, J.G., Dymond, J.R., 1988. How much do trees reduce landsliding? J. Soil Water Conserv. 43 (6), 495–498.

Hicks, D.L., 1989a. Farm conservation measures' effect on hill country erosion: an assessment in the wake of Cyclone Bola. In: DSIR Land and Soil Sciences Technical Record PN 3. Palmerston North, DSIR.

Hicks, D.L., 1989b. Storm damage to bush, pasture and forest: some evidence from Cyclone Bola. In: DSIR Land Resources Technical Record PN2. Palmerston North, DSIR.

Hicks, D.L., 1992. Impact of soil conservation on storm-damaged hill grazing lands in New Zealand. Australian Journal of Soil and Water Conservation 5, 34–40.

Hicks, D.M., Shankar, U., McKerchar, A.I., Basher, L., Jessen, M., Lynn, I., Page, M., 2011. Suspended sediment yields from New Zealand rivers. J. Hydrol. 50, 81–142.

Hölbling, D., Betts, H., Spiekermann, R., Phillips, C., 2016. Identifying spatio-temporal landslide hotspots on North Island, New Zealand, by analysing historical and recent aerial photography. Geosciences 6, 48.

Istanbulluoglu, Erkan, Bras L., Rafael, 2005. Vegetation-modulated landscape evolution: Effects of vegetation on landscape processes, drainage density, and topography. J. Geophys. Res.: Earth Surf. 110 (2), 1–19. https://doi.org/10.1029/2004JF000249.

Kanungo, D., Arora, M., Sarkar, S., Gupta, R., 2009. Landslide susceptibility zonation (LSZ) mapping — a review. J. South Asia Disaster Stud. 2 (1), 81–105.

Kemp, P.D., Hawke, M.F., Knowles, R.L., 2018. Temperate agroforestry systems in New Zealand. In: Gordon, A.M., Newman, S.M., Coleman, B.R.W. (Eds.), Temperate Agroforestry Systems. CABI, pp. 224–236.

Knevels, Raphael, Petschko, Helene, Proske, Herwig, Leopold, Philip, Douglas, Maraun, Brenning, Alexander, et al., 2020. Event-Based Landslide Modeling in the Styrian Basin , Austria : Accounting for Time-Varying Rainfall and Land Cover. Geosciences 10 (2017), 1–29. https://doi.org/10.3390/geosciences10060217.

Kuhn, M., 2008. Caret package. J. Stat. Software 28 (5).

Lambert, M.G., Trustrum, N.A., Costall, D.A., 1984. Effect of soil slip erosion on seasonally dry wairarapa hill pastures. N. Z. J. Agric. Res. 27 (1), 57–64. https://doi.org/10.1080/00288233.1984.10425732.

Lambert, M.G., Trustrum, N.A., Costall, D.A., Foote, A.G., 1993. Revegetation of landslide scars in Wairarapa hill country. Proc. N. Z. Grassl. Assoc. 55, 177–181.

Lefsky, M.A., Cohen, W.B., Acker, S.A., Parker, G.G., Spies, T.A., Harding, D., 1999. Lidar remote sensing of the canopy structure and biophysical properties of douglas-fir western hemlock forests. Remote Sens. Environ. 70, 339–361.

Mackay, A., Douglas, G., Wheeler, D., Power, I., 2012. Establishing a common framework for Regional Councils to assess, quantifying and reporting on the effectiveness of soil conservation works on potential farm erosion risk and sediment loss. In: Report for Horizons Regional Council under Envirolink Medium Advice Grant HZLC87, AgResearch. Palmerston North.

Mackay-Smith, T.H., Burkitt, L.L., López, I.F., Reid, J., Philips, C.J., (submitted). Silvopastoral properties of kānuka (*Kunzea* spp.) and poplar (*Populus* spp.) in New Zealand hill country. J. Environ. Manag..

Manderson, A.K., Mackay, A.D., Palmer, A.P., 2007. Environmental whole farm management plans: their character, diversity, and use as agri-environmental indicators in New Zealand. J. Environ. Manag. 82 (3), 319–331.

McIvor, I.R., Douglas, G.B., Hurst, S.E., Hussain, Z., Foote, A.G., 2008. Structural root growth of young Veronese poplars on erodible slopes in the southern North Island, New Zealand. Agrofor. Syst. 72 (1), 75–86. https://doi.org/10.1007/s10457-007-9090-5.

McIvor, I.R., Douglas, G.B., Benavides, R., 2009. Coarse root growth of Veronese poplar trees varies with position on an erodible slope in New Zealand. Agrofor. Syst. 76 (1), 251–264. https://doi.org/10.1007/s10457-009-9209-y.

McIvor, I., Douglas, G., Dymond, J., Eyles, G., Marde, M., 2011. Pastoral hill slope erosion in New Zealand and the role of poplar and willow trees in its reduction. Soil Erosion Issues in Agriculture. https://doi.org/10.5772/24365.

McIvor, I., Clarke, K., Douglas, G., 2015. Effectiveness of conservation trees in reducing erosion following a storm event. In: Currie, L.D., Burkitt, L.L. (Eds.), Proceedings, 28th Annual Fertiliser and Lime Research Centre Workshop 'Moving Farm Systems to Improved Attenuation', 8–9 February 2007. Occasional Report 28. Palmerston North, Fertiliser and Lime Research Centre.

Moos, C., Bebi, P., Graf, F., Mattli, J., Rickli, C., Schwarz, M., 2016. How does forest structure affect root reinforcement and susceptibility to shallow landslides? Earth Surf. Process. Landforms 41 (7), 951–960. https://doi.org/10.1002/esp.3887.

Norton, D.A., Suryaningrum, F., Buckley, H.L., Case, B.S., Hamish Cochrane, C., Forbes, A.S., Harcombe, M., 2020. Achieving win-win outcomes for pastoral farming and biodiversity conservation in New Zealand. N. Z. J. Ecol. 44 (2) https://doi.org/10.20417/nzjecol.44.15.

Phillips, C.J., Marden, M., 2005. Reforestation schemes to manage regional landslide risk. In: Glade, T., Anderson, M., Crozier, M.J. (Eds.), Landslide Hazard and Risk. John Wiley, Chichester, pp. 517–547.

Phillips, C.J., Watson, A.J., 1994. Structural tree root research in New Zealand. In: Landcare Research Science Series No. 7. Manaaki Whenua Press, Lincoln, New Zealand, p. 71.

Phillips, C.J., Marden, M., Miller, D., 2000. Review of plant performance for erosion control in the East Coast region. In: Landcare Research Contract Report LC9900/111 for MAF Policy.

Phillips, C., Marden, M., Douglas, G., McIvor, I., Ekanayake, J., 2008. Decision support for sustainable land management: effectiveness of wide-spaced trees. In: Landcare Research Contract Report LC0708/126 for Ministry of Agriculture and Forestry.

Phillips, C.J., Ekanayake, J.C., Marden, M., 2011. Root site occupancy modelling of young New Zealand native plants: implications for soil reinforcement. Plant Soil 346 (1), 201–214. https://doi.org/10.1007/s11104-011-0810-2.

Phillips, C.J., Marden, M., Suzanne, L.M., 2014. Observations of root growth of young poplar and willow planting types. N. Z. J. For. Sci. 44 (1), 1–12. https://doi.org/10.1186/s40490-014-0015-6.

Phillips, C.J., Marden, M., Basher, L.R., 2018. Geomorphology and forest management in New Zealand's erodible steeplands: an overview. Geomorphology 307, 107–121. https://doi.org/10.1016/j.geomorph.2017.07.031.

Pirotti, F., Kobal, M., Roussel, J.R., 2017. A comparison of tree segmentation methods using very high density airborne laser scanner data. Int. Arch. Photogram. Rem. Sens. Spatial Inf. Sci. 42, 285–290.

Reichenbach, P., Rossi, M., Malamud, B.D., Mihir, M., Guzzetti, F., 2018. A review of statistically-based landslide susceptibility models. Earth Sci. Rev. 180 (March), 60–91. https://doi.org/10.1016/j.earscirev.2018.03.001.

Romeijn, J., 2009. Statistics as inductive inference. In: EPRINTS-BOOK. TITLE University of Groningen.

Rosser, B.J., Ross, C.W., 2011. Recovery of pasture production and soil properties on soil slip scars in erodible siltstone hill country, Wairarapa, New Zealand. N. Z. J. Agric. Res. 54 (1), 23–44. https://doi.org/10.1080/00288233.2010.535489.

Sakals, M.E., Sidle, R.C., 2004. A spatial and temporal model of root cohesion in forest soils. Can. J. For. Res. 34 (4), 950–958. https://doi.org/10.1139/x03-268.

Salvatici, Teresa, Tofani, Veronica, Rossi, Guglielmo, D'Ambrosio, Michele, Stefanelli T, Carlo, Masi B, Elena, Rosi, Ascanio, Pazzi, Vannocci, Petrolo, Miriana, Catani, Filippo, Ratto, Sara, Stevenin, Hervè, Casagli, Nicola, et al., 2018. Application of a physically based model to forecast shallow landslides at a regional scale. Nat. Hazards Earth Syst. Sci. 18 (7), 1919–1935. https://doi.org/10.5194/nhess-18-1919-2018.

Schmidt, K.M., Roering, J.J., Stock, J.D., Dietrich, W.E., Montgomery, D.R., Schaub, T., 2001. The variability of root cohesion as an influence on shallow landslide susceptibility in the Oregon Coast Range. Can. Geotech. J. 38 (5), 995–1024.

Schwarz, M., Preti, F., Giadrossich, F., Lehmann, P., Or, D., 2010a. Quantifying the role of vegetation in slope stability: a case study in Tuscany (Italy). Ecol. Eng. 36 (3), 285–291. https://doi.org/10.1016/j.ecoleng.2009.06.014.

Schwarz, M., Lehmann, P., Or, D., 2010b. Quantifying lateral root reinforcement in steep slopes - from a bundle of roots to tree stands. Earth Surf. Process. Landforms 35 (3), 354–367.

Schwarz, M., Cohen, D., Or, D., 2012. Spatial characterization of root reinforcement at stand scale: theory and case study. Geomorphology 171–172. https://doi.org/10.1016/j.geomorph.2012.05.020, 190–200.

Schwarz, M., Phillips, C., Marden, M., McIvor, I.R., Douglas, G.B., Watson, A., 2016. Modelling of root reinforcement and erosion control by 'Veronese' poplar on pastoral hill country in New Zealand. N. Z. J. For. Sci. 46 (1), 1–17. https://doi.org/10.1186/s40490-016-0060-4.

Smale, M.C., McLeod, M., Smale, P.N., 1997. Vegetation and soil recovery on shallow landslide scars in tertiary hill country, East Cape Region, New Zealand. N. Z. J. Ecol. 21 (1), 31–41.

Stokes, A., Atger, C., Bengough, A.G., Fourcaud, T., Sidle, R.C., 2009. Desirable plant root traits for protecting natural and engineered slopes against landslides. Plant Soil 324, 1–30.

Stone, E.L., Kalisz, P.J., 1991. On the maximum extent of tree roots. For. Ecol. Manag. 46, 59–102.

Suzen, M.L., Kaya, B.S., 2011. Evaluation of environmental parameters in logistic regression models for landslide susceptibility mapping. International Journal of Digital Earth 5, 338–355.

Temgoua, A.G.T., Kokutse, N.K., Kavazović, Z., 2016. Influence of forest stands and root morphologies on hillslope stability. Ecol. Eng. 95, 622–634. https://doi.org/10.1016/j.ecoleng.2016.06.073.

Thompson, R.C., Luckman, P.G., 1993. Performance of biological erosion control in New Zealand soft rock hill terrain. Agrofor. Syst. 21, 191–211.

Torabzadeh, H., Leiterer, R., Hueni, A., Schaepman, M.E., Morsdorf, F., 2019. Tree species classification in a temperate mixed forest using a combination of imaging spectroscopy and airborne laser scanning. Agric. For. Meteorol. 279 (September), 107744. https://doi.org/10.1016/j.agrformet.2019.107744.

Van Den Eeckhaut, M., Reichenbach, P., Guzzetti, F., Rossi, M., Poesen, J.A., 2009. Combined landslide inventory and susceptibility assessment based on different mapping units: an example from the Flemish Ardennes, Belgium. Nat. Hazards Earth Syst. Sci. 9 (2), 507–521. https://doi.org/10.5194/nhess-9-507-2009.

van Kraayenoord, C.W.S., Hathaway, R.L., 1986. Plant Materials Handbook for Soil Conservation. In: Principles and Practices, ume 1. National Water and Soil Conservation Authority, Wellington, New Zealand.

van Noordwijk, M., Hairiah, K., Tata, H.L., Lasco, L., 2019. How can agroforestry be part of disaster risk management? In: van Noordwijk, M. (Ed.), Sustainable Development through Trees on Farms: Agroforestry in its Fifth Decade. Bogor, Indonesia: World Agroforestry (ICRAF) Southeast Asia Regional Program, pp. 251–267.

van Westen, C.J., Castellanos, E., Kuriakose, S.L., 2008. Spatial data for landslide susceptibility, hazard, and vulnerability assessment: an overview. Eng. Geol. 102 (3–4), 112–131. https://doi.org/10.1016/j.enggeo.2008.03.010.

Watson, A.L., Marden, M., 2004. Live root-wood tensile strengths of some common New Zealand indigenous and plantation tree species. NZ J. For Sci 34, 344–353.

Watson, A., O'Loughlin, C., 1990. Structural root morphology and biomass of the three age-classes of Pinus Radiata. N. Z. J. For. Sci. 20, 97–110.

Watson, A., Marden, M., Rowan, D., 1995. Tree species performance and slope stability. In: Barker, D.H. (Ed.), Vegetation and Slope Stabilisation, Protection and Ecology. Thomas Telford Press, p. 161—171.

Watson, A., Phillips, C., Marden, M., 1999. Root strength, growth, and rates of decay: root reinforcement changes of two tree species and their contribution to slope stability. Support. Roots Trees Woody Plants Form. Funct. Physiol. 217, 41–49.

Weinstein, B.G., Marconi, S., Bohlman, S., Zare, A., White, E., 2019. Individual tree-crown detection in rgb imagery using semi-supervised deep learning neural networks. Rem. Sens. 11 (11), 1–13. https://doi.org/10.3390/rs11111309.

Weinstein, B.G., Marconi, S., Bohlman, S.A., Zare, A., White, E.P., 2020a. Cross-site learning in deep learning RGB tree crown detection. Ecol. Inf. 56 (January), 101061. https://doi.org/10.1016/j.ecoinf.2020.101061.

Weinstein, B.G., Marconi, S., Bohlman, S., Zare, A., Singh, A., Graves, S.J., White, E., 2020b. NEON Crowns: a remote sensing derived dataset of 100 million individual tree crowns. BioRxiv. https://doi.org/10.1101/2020.09.08.287839, 2020.09.08.287839.

Wilkinson, A., 1999. Poplars and willows for soil erosion control in New Zealand. Biomass Bioenergy 16 (4), 263–274. https://doi.org/10.1016/S0961-9534(99)00007-0.

Zhen, Z., Quackenbush, L., Zhang, L., 2016. Trends in automatic individual tree crown detection and delineation—evolution of LiDAR data. Rem. Sens. 8, 333.

Zillgens, B., Merz, B., Kirnbauer, R., Tilch, N., 2007. Analysis of the runoff response of an alpine catchment at different scales. Hydrol. Earth Syst. Sci. 11, 1441–1454.

Zörner, J., Dymond, J.R., Shepherd, J.D., Wiser, S.K., Jolly, B., 2018. LiDAR-based regional inventory of tall trees-Wellington, New Zealand. Forests 9 (11), 1–16. https://doi.org/10.3390/f9110702.

Smith H.G., Spiekermann R.I., Betts H., Neverman A.J. 2021. Comparing methods of landslide data acquisition for susceptibility modelling: examples from New Zealand. Geomorphology. In press. https://doi.org/10.1016/j.geomorph.2021.107660.